USAARL-TECH-FR--2026-32

UNITED STATES ARMY AEROMEDICAL RESEARCH LABORATORY

Evaluation of Aeromedical Patient Movement Systems in Vertical Accelerative Exposures for the Development of A Dynamic Test Standard

Danielle Rhodes, Michael Schlick, Blake Johnson, Joseph Willett, Lucia Melara, Shawn Boons, & B. Joseph McEntire

Notice

Qualified Requesters

Qualified requesters may obtain copies from the Defense Technical Information Center (DTIC), Fort Belvoir, Virginia 22060. Orders will be expedited if placed through the librarian or other person designated to request documents from DTIC.

Change of Address

Organizations receiving reports from the U.S. Army Aeromedical Research Laboratory on automatic mailing lists should confirm correct address when corresponding about laboratory reports.

Disposition

Destroy this document when it is no longer needed. Do not return it to the originator.

Disclaimer

The views, opinions, and/or findings contained in this report are those of the author(s) and should not be construed as an official Department of the Army position, policy, or decision, unless so designated by other official documentation. Citation of trade names in this report does not constitute an official Department of the Army endorsement or approval of the use of such commercial items.

REPORT DOCUMENTATION PAGE	*Form Approved* *OMB No. 0704-0188*

1. REPORT DATE *(DD-MM-YYYY)*	2. REPORT TYPE	3. DATES COVERED *(From - To)*
08-14-2026	Final Report	10/1/2022-9/30/2025

4. TITLE AND SUBTITLE

Evaluation of Aeromedical Patient Movement Systems in Vertical Accelerative Exposures for the Development of A Dynamic Test Standard

5a. CONTRACT NUMBER

5b. GRANT NUMBER

5c. PROGRAM ELEMENT NUMBER

0602787A

6. AUTHOR(S)

Rhodes, D.,[1,2], Schlick, M.[1,2], Johnson, B.[1,2], Willett, J.[1,2], Melara, L.[1,2], Booms, S.[1], & McEntire, B. J.[1]

5d. PROJECT NUMBER

MM4

5e. TASK NUMBER

CC04

5f. WORK UNIT NUMBER

7. PERFORMING ORGANIZATION NAME(S) AND ADDRESS(ES)

U.S. Army Aeromedical Research Laboratory
P.O. Box 620577
Fort Rucker, AL 36362

8. PERFORMING ORGANIZATION REPORT NUMBER

USAARL-TECH-FR--2026-32

9. SPONSORING/MONITORING AGENCY NAME(S) AND ADDRESS(ES)

U.S. Army Medical Research and Development Command
Military Operational Medicine Research Program
810 Schreider Street
Fort Detrick, MD 21702

10. SPONSOR/MONITOR'S ACRONYM(S)

USAMRDC MOMRP

11. SPONSOR/MONITOR'S REPORT NUMBER(S)

12. DISTRIBUTION/AVAILABILITY STATEMENT

DISTRIBUTION STATEMENT A. Approved for public release: distribution is unlimited.

13. SUPPLEMENTARY NOTES

[1]Chenega Corporation; [2]U.S. Army Aeromedical Research Laboratory

14. ABSTRACT

Protection and survival of aircraft occupants during mishaps should be primary considerations in the design, development, and testing of aeromedical patient movement systems (APMS). All patients being transported, need to have crashworthy litters that will minimize additional injuries during a mishap. The Aircraft Crash Survival Design Guide (ACSDG) recommends a 48 G pure vertical dynamic test (Desjardins et al., 1989); however, dynamic loading specifications do not exist for military patient litters and APMS are not required to meet recommended crashworthy standards for patient safety. Litter system collapse and failure during crash conditions can expose patients, medical attendants, and nearby occupants to additional hazards and injury mechanisms. The objective of this research was to demonstrate the need for the development of a comprehensive vertical dynamic test standard with dynamic test conditions using the USAARL Vertical Acceleration Tower (VAT).

15. SUBJECT TERMS

Litter, dynamic testing, crashworthy litters, crashworthiness, dynamic test standards, anthropomorphic test device, ATD

16. SECURITY CLASSIFICATION OF: a. REPORT	b. ABSTRACT	c. THIS PAGE	17. LIMITATION OF ABSTRACT	18. NUMBER OF PAGES	19a. NAME OF RESPONSIBLE PERSON
UNCLAS	UNCLAS	UNCLAS	SAR	43	Amanda Hayes, MS
					19b. TELEPHONE NUMBER *(Include area code)* 334-255-6067

REPORT DOCUMENTATION PAGE (SF298)
(Continuation Sheet)

14. Abstract (continued)

The instrumented Hybrid III 95th percentile male anthropomorphic test device (ATD) with a Pedestrian Pelvis (HIII-95M-Ped) and APMS (floor-mounted and elevated) were exposed to two vertical accelerative test severities targeting 7 G and 23 G to evaluate the structural integrity of the APMS and ATD response. Test results demonstrated that even at the lower test severity, deformation of the APMS components was noted and high speed video and sensor analysis confirmed the ATD chest, pelvis, and knees impacted the surface below the litter during the test, indicating a potential increase in injury severity of a patient in a mishap. Preliminary data resulting from this study demonstrates a need for an APMS dynamic testing requirement. Furthermore, floor-mounted and elevated APMS may need to be evaluated differently due to structural differences. Future work should include dynamic APMS tests in multiple loading scenarios with post-mortem human subjects to assess ATD biofidelity in the supine position.

Executive Summary

Protection and survival of aircraft occupants during mishaps should be considered during the design, development, and testing of aeromedical patient movement systems (APMS). An APMS consists of the litter and any components used to secure the litter and litter occupant in the aircraft. The rotary-wing APMS can be floor-mounted across the aircraft or elevated, allowing multiple patients to be vertically stacked against the wall of the aircraft. All patients should be transported using crashworthy litters that will minimize additional injuries during a mishap. Additionally, APMS that collapse and fail during crash conditions expose all nearby occupants to additional hazards and injury mechanisms. The Aircraft Crash Survival Design Guide recommends subjecting the litter to a triangular shaped acceleration pulse with a peak acceleration of 48 G (where G is the standard acceleration due to earth's gravity [32.174 feet/second squared (ft/s^2)]) and a 42 feet/second (ft/s) velocity change in pure vertical dynamic test (Desjardins et al., 1989) for APMS; however, dynamic loading specifications do not exist for military APMS or their components and the APMS or its subcomponents are not required to meet the recommended crashworthy standards for patient safety. The objective of this research was to use the Vertical Acceleration Tower at the U.S. Army Aeromedical Research Laboratory to demonstrate the need for the development of a comprehensive vertical dynamic test standard for litters and recommend dynamic test conditions. Two APMS configurations, floor-mounted and elevated, were tested. The APMS contained an instrumented Hybrid III 95th percentile male anthropomorphic test device (ATD) with a Pedestrian Pelvis as a simulated patient. The two configurations were exposed to two vertical accelerative test severities targeting 7 G and 23 G to evaluate the structural integrity of the APMS and ATD response. Test results demonstrated that deformation of the APMS components occurred even at the lower test severity. High speed video and sensor analyses confirmed that the ATD chest, pelvis, and knees impacted the surface below the litter during all tests, indicating a potential to introduce new injuries or exacerbate an existing injury for a patient in a mishap. Preliminary data resulting from this study demonstrated the need for an APMS dynamic testing requirement. Furthermore, floor-mounted and elevated APMS may need to be evaluated differently due to structural differences. Future work should include dynamic APMS tests in multiple loading scenarios with post-mortem human subjects to assess ATD biofidelity in the supine position.

The outcomes of this research led to the following recommendations:

- A static and dynamic test standard for APMS assessment should be developed for multiple loading conditions (i.e., vertical, longitudinal, and lateral).
- The HIII-95M-PED is recommended for static litter performance requirements.
- The HIII-50M-PED is recommended for dynamic litter performance requirements.
- At a minimum, the acceleration pulse for the APMS vertical dynamic test should be 23 G at a velocity of 25 ft/s.
- Minimum instrumentation should consider an accelerometer on the carriage, 6DOF on the litter poles above each stirrup, and the standard HIII-50M-PED instrumentation package.
- It is recommended that securing the stirrups to the surface below the litter be considered.
- Additional research should be conducted to develop injury risk criteria for supine occupants transported in APMS.

This page is intentionally blank.

Acknowledgments

The authors would like to thank Nathan Flath for APMS fixture design, Joseph Parish and Amanda Warren for assistance with instrumentation and data collections, and Jeremy Latham for assisting with test setup and pulse development. Steven Arntzen was instrumental in scanning the litters pre- and post- test to document deformation. We would also like to acknowledge Lauren Watts for her help with testing documentation and execution.

This page is intentionally blank.

Table of Contents

Page

Executive Summary ... iii
Acknowledgments ... v
Introduction ... 1
Methods ... 4
    Litter Configurations and ATD Selection ... 4
    Coordinate Systems ... 10
    Pulse Development ... 11
    Instrumentation ... 12
    Data Collection ... 13
Results ... 14
    Floor-Mounted APMS ... 14
    Elevated APMS ... 24
Discussion ... 35
Conclusion ... 38
Recommendations ... 38
References ... 40
Appendix ... 42

List of Figures

1. The collapse of the litter system during the full-scale dynamic crash test of the CH-46 was catastrophic. The test setup included three litters, each containing an ATD, mounted on a stanchion litter system. The APMS is pictured pre-impact (A). The position of the litter system and ATDs during the impact event is also shown (B). ... 3
2. The Talon II 90C litters used for this study consisted of a webbing expanded between two litter poles (A). The bottom view of the litter shows the left and right stirrups and spreader bar (B). ... 4
3. The arms were disarticulated at the shoulder to avoid artificial rigid contact of the ATD shoulder bracket with the litter poles. An orange strap was passed through the arm opening of the ATD chest jacket to tether the arms. ... 5
4. Floor-mounted (A) and elevated platform (B) APMS fixturing was designed for the VAT. ... 6
5. The floor-mounted APMS consisted of a litter with two integrated occupant straps (blue) securing the ATD to the litter and three straps (green) securing the APMS and patient to a track in the simulated aircraft floor with quick disconnect adapters (indicated by yellow ovals). ... 7
6. The elevated APMS components (not pictured in Figure 4) that connected to the simulated airframe to support the litter pan and litter. ... 8

Table of Contents (continued)

List of Figures (continued)

Page

7. The elevated APMS configuration consisted of a litter with two integrated occupant straps (blue) that secured the ATD to the litter and three straps (green) with quick disconnect adapters (indicated by yellow ovals) that attached underneath the elevated litter pan to secure the litter and ATD. A third occupant strap (yellow) was added around the lower legs of the ATD and the litter to remain consistent with the floor-mounted APMS restraints and prevent the legs from flailing. 9
8. The ATD placed in the elevated configuration during both APMS configurations is shown. 9
9. The CS of the ATD and the APMS were consistent with the 2007 version of the SAE J-211-1 guidelines and the ACSDG, respectively. 10
10. The litter was instrumented with four five-degree-of-freedom (5DOF) accelerometers and an angular rate sensor package (red). The straps were instrumented with restraint load cells (orange). Blue straps secured the ATD to the litter and green straps secured the ATD and litter into the APMS. The floor-mounted configuration (A) had five straps (blue and green). The elevated configuration (B) also had five straps (blue and green) but, due to geometry, an extra un-instrumented strap (yellow) was used to prevent lower extremity flail. 12
11. The elevated APMS was instrumented with two accelerometers centered on the bottom of the litter pan (green) under the chest and lower extremities of the ATD. One accelerometer was also mounted to the end of each litter support arm (yellow). 13
12. The floor-mounted APMS was exposed to targeted 7 G and 23 G pulses. Carriage acceleration and time were recorded for the six tests. 14
13. Carriage, ATD head, chest, and pelvis, and the four litter pole acceleration versus time data from one of the 7 G pulses for the floor-mounted APMS test were plotted. A small initial delay between the carriage acceleration and the litter poles, indicated by the red arrow, was noted. 15
14. Carriage, ATD head, chest, and pelvis, and the four litter pole acceleration versus time data from one of the 23 G pulses for the floor-mounted APMS test were plotted. A small initial delay between the carriage acceleration and the litter poles, indicated by the red arrow, was noted. 16
15. Forces in the x-, y-, and z- direction versus time data from one of the 7 G and 23 G pulses for the floor-mounted APMS test was plotted. 17
16. Moments in the x-, y-, and z- direction versus time data from one of the 7 G and 23 G pulses for the floor-mounted APMS test was plotted. 18

Table of Contents (continued)

List of Figures (continued)

Page

17. Views from the two cameras centered on the head/chest and lower extremities were combined to present a full-body image of the 23 G pulse. A time-zero frame (A), a frame where contact was observed (B), and a frame showing the rebound of the ATD (C) were selected from the HSV data for the floor-mounted APMS. 20
18. The ATD impacted the simulated aircraft floor during all pulses (imprint after one of the 23 G pulses is shown). 21
19. Bottom view (A) and side view (B) scans of the litter were taken of the floor-mounted APMS litter bottom to document webbing and component deformation after one of the 23 G pulses. Units of deformation in the legend are in millimeters. 22
20. Pre-test photographs show the intact floor-mounted APMS spreader bars (yellow arrows) of the head (A) and foot (B). Deformation of the head (C) and foot (D) spreader bars (yellow arrows) after one of the 23 G pulses were noted post-test. 23
21. The elevated APMS was exposed to targeted 7 G and 23 G pulses. 24
22. Carriage, ATD head, chest, and pelvis, and the four litter pole accelerations versus time data from one of the 7 G pulses for the elevated APMS were plotted. It was noted that the initial accelerometer data delay was smaller for the litter poles nearest the supporting simulated airframe (patient left) than the litter poles furthest away (patient right). 25
23. Carriage, ATD head, chest, and pelvis, and the four litter pole accelerations versus time data from one of the 23 G pulses for the elevated APMS were plotted. There was an initial accelerometer data delay, indicated by the red arrow, that was smaller for the litter poles nearest the supporting simulated airframe (patient left) than the litter poles furthest away (patient right). 26
24. Force in the x-, y-, and z- direction versus time data from one of the 7 G and 23 G pulses for the elevated APMS test were plotted...27
25. Moment in the x-, y-, and z- direction versus time data from one of the 7 G and 23 G pulses for the elevated APMS test were plotted...28
26. Views from the two HSV cameras centered on the head/chest (left) and pelvis/lower extremities (right) were combined for the 23 G pulse. The time-zero frame (A), frame where contact was observed (B), and the frame showing the rebound of the ATD (C) were selected from the HSV data for the elevated APMS. 30
27. The ATD made contact with the litter pan during all pulses (imprint after one of the 23 G pulses is shown). 31
28. Bottom view (A) and side view (B) scans of the litter were taken of the elevated APMS litter bottom to document canvas and component deformation after one of the 23 G pulses. Units of deformation in the legend are in millimeters. 32
29. Pre-test photographs show the intact elevated APMS spreader bars of the head (A) and foot (B). Deformation of the head (C) and foot (D) spreader bars after the medium pulse were noted. 33
30. A straight edge was used to note pin deformation in the forward and aft litter pan support after the 23 G pulse. The red line shows the deformation from the straight edge. 34
31. The elevated litter pan has a hinged construction (arrows). 36

Table of Contents (continued)

List of Tables

Page

1. Average Peak ATD Accelerations for the Head, Chest, and Pelvis in the x-Axis Direction for the Floor-Mounted APMS Configuration 19
2. Average Peak ATD Right and Left Femur Load Cell Force in the x-Axis and Moment in the y-Axis Directions for the Floor-Mounted APMS Configuration 19
3. Average Peak ATD Accelerations for the Head, Chest, and Pelvis in the x-Axis Direction for the Elevated APMS Configuration 28
4. Average Peak ATD Right and Left Femur Load Cell Force in the x-Axis and Moment in the y-Axis Directions for the Elevated APMS Configuration 29
A1. Peak ATD Accelerations for the Head, Chest, and Pelvis in the x-Axis Direction for the Floor-Mounted APMS Configuration 42
A2. Peak ATD Right and Left Femur Load Cell Force in the x-Axis Direction for the Floor-Mounted APMS Configuration 42
A3. Peak ATD Accelerations for the Head, Chest, and Pelvis in the x-Axis Direction for the Elevated APMS Configuration 43
A4. Peak ATD Right and Left Femur Load Cell Force in the x-Axis Direction for the Elevated APMS Configuration 43

Introduction

Several advancements have been made in protecting and treating the injured Soldier through aeromedical support. In 1920, the U.S. Army built and flew the first aircraft designed as an ambulance. The DeHavilland (DH-4A) had room for a pilot, two litter patients, and a medical attendant, providing faster access to medical treatment (Dorland & Nanney, 1982). A military specification, MIL-A-8865 (AS), Airplane Strength and Rigidity Miscellaneous Loads, was published in 1960 and updated in 1987 (Department of Defense [DoD], 1987), that specifies the parameters to use when statically testing aeromedical patient movement systems (APMS). Weinberg (1966) conducted a full-scale dynamic crash test of a CH-21 helicopter with standard H-21 rotary-wing litter installation designed to MIL-A-8865 (AS) requirements. Weinberg (1966) noted that the specification did not require combined loading of the individual components. Furthermore, the results concluded that the current litter systems designed to MIL-A-8865 (AS) would fail under moderate impact conditions and subject the patients to amplified accelerations and contact injuries. The original Crash Survival Design Guide (CSDG), published in 1967, consolidated the design criteria for the improved crashworthiness of seats and litters in U.S. Army aircraft, and formally communicated the test parameters and performance required to improve occupant survivability (Turnbow et al., 1967). Unfortunately, the first publication of the CSDG upheld the static litter installation load test standards outlined in MIL-A-8865 (AS), despite the findings and recommendations of Weinberg (1966). Twenty years later, litter installation loading requirements were updated in MIL-A-8865B (AS) by the Naval Air Systems Command; however, the static and dynamic testing requirements were not revised (DoD, 1987).

Protection and survival of aircraft occupants during mishaps should be primary considerations in the design, development, and testing of APMS. The CSDG was last updated in 1989 as a five-volume document and renamed the Aircraft Crash Survival Design Guide (ACSDG). This revision evolved to incorporate dynamic test and performance requirements for seats and litters (Desjardins et al., 1989). The recommended requirements were developed from aircraft crash resistance research conducted between 1960 and 1987 to improve occupant survivability (Desjardins et al., 1989). The current version of the ACSDG (Volume 4) outlines the current design criteria for litters and their attachment systems (Section 4) and includes static requirement recommendations (Section 10) with a description of static load-deflection tests for longitudinal, vertical, and lateral directions (Desjardins et al., 1989). Section 10 of the ACSDG also recommends a single vertical dynamic test evaluation of the litter occupied by a 95th percentile anthropomorphic test device (ATD), plus clothing and personal gear, a splint or cast, a litter, and support bracket for a total weight of 250 pounds (lb). This test should subject the occupant to a triangular acceleration pulse of 48 G (where G is the standard acceleration due to earth's gravity [32.174 feet/second squared (ft/s^2)]) for a 0.054 second (s) duration to achieve a 42 ft/s velocity change. Additionally, the ACSDG recommended three accelerometers be installed in the ATD’s head, chest, and pelvic regions and oriented to sense the accelerations in the vertical direction.

Furthermore, military standards and specifications have not been updated with more recent Solder anthropometry reported in ANSUR II (Gordon et al., 2014) and equipment weights (Rhodes et al., 2021). Rhodes et al. (2021) concluded that the additional weight of the occupant and equipment would decrease the aircraft accelerative loading that the seat could withstand. Consequently, this finding logically extends to APMS.

As APMS users identified needs for improving aviation crash survivability, studies were performed to increase the breadth and understanding of Soldier and personnel viability after survivable crashes (National Transportation Safety Board [NTSB], 1980). The first full-scale dynamic crash test of a CH-21 helicopter containing an APMS was performed in 1962 (Schamadan et al., 1963). During this test, a 50 G vertical acceleration was recorded at the pelvis of the ATD in the lower APMS as the pelvis bottomed out against the aircraft floor. This test concluded that the APMS was not capable of providing adequate patient protection in potentially survivable crashes (Schamadan et al., 1963). A second crash test of a CH-21 configured with an APMS was tested in 1963 and yielded similar results and conclusions (Weinberg, 1966). Additionally, researchers at the U.S. Army Aeromedical Research Laboratory (USAARL) performed a quasi-static load-deformation evaluation of three U.S. Army litters (not systems) while supported by the handles, stanchions, and stirrups (Logsdon et al., 2015). The performance of the three litters met static performance requirements; however, given the significant amount of litter flexure under tested loads, researchers were concerned that the recorded litter deformation could result in occupant impact with the underlying structure in a survivable crash, potentially causing further injury to the patient.

In 2014, researchers at USAARL in collaboration with National Aeronautics and Space Administration (NASA) instrumented and recorded a pair of controlled, survivable, full-scale crash tests of CH-46 helicopters to assess the crashworthiness of a legacy triple stack litter system (Annett et al., 2014; Annett & Littell, 2015). During the first CH-46 crash test, the APMS, using the U.S. Army decontaminable and Talon II litters, was unable to maintain structural integrity during the crash, resulting in catastrophic structural failures of the litters and support system with litter occupant displacement (Weisenbach et al., 2017). For the second CH-46 test, modifications were made to strengthen the litter support system and occupant retention systems that reduced pre-crash patient displacement and flail; however, the litters and support system experienced similar catastrophic structural failures (Figure 1) (McEntire et al., 2016; Weisenbach et al., 2017). However, it is not known how the measured ATD responses correlate with injury risk. Both CH-46 tests revealed the limitations of the legacy triple stack litter support system and illustrated the need for a significant design improvement regarding occupant protection of litter-borne occupants (Weisenbach et al., 2017).

This space is intentionally blank.

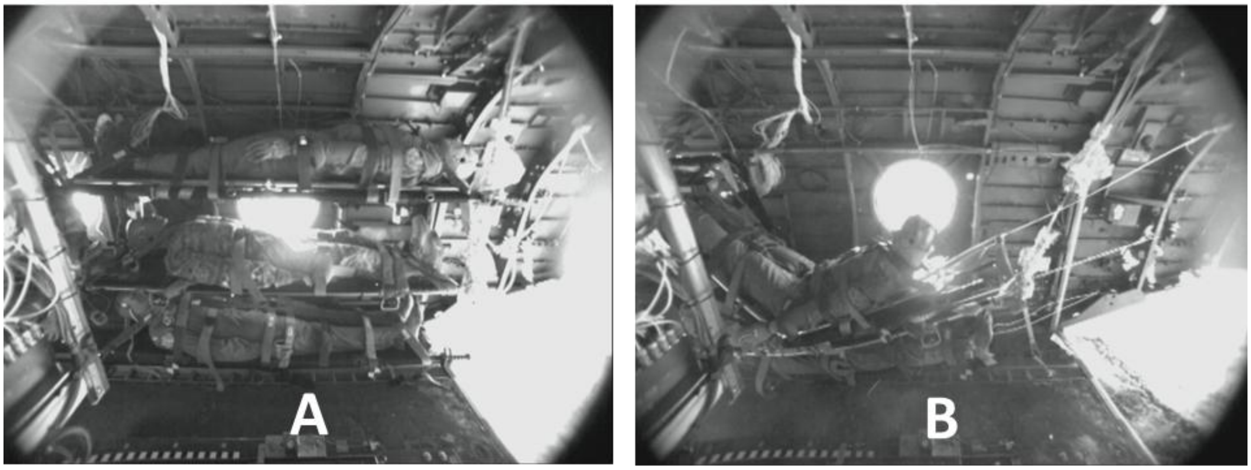

Figure 1. The collapse of the litter system during the full-scale dynamic crash test of the CH-46 was catastrophic. The test setup included three litters, each containing an ATD, mounted on a stanchion litter system. The APMS is pictured pre-impact (A). The position of the litter system and ATDs during the impact event is also shown (B).

Future combat scenarios of multi-domain operations (MDOs) against near-peer type adversaries are anticipated to result in increased risks for medical evacuation (MEDEVAC) missions, crews, and patients. Future MDOs will likely increase the risk of mishaps and shoot-down events as helicopter missions will include flights at lower altitudes and higher speeds (Department of the Army, 2018; U.S. Army Medical Department Center & School, 2019). MEDEVAC missions are frequently conducted in environments that are known to pose increased risks of flight mishaps or exposure to shoot-down threats (e.g., enemy fire, poor weather, low visibility, etc.). These adverse events increase the injury risk to the aircraft occupants, including the patients.

Currently, dynamic loading performance requirements do not exist for military patient litters and APMS are not required to meet recommended crashworthy standards for increased patient safety. Litter system collapse and failure during crash conditions expose all nearby occupants to additional hazards and injury mechanisms. The objectives of this research were to demonstrate the need for the development of a comprehensive dynamic test standard by using the USAARL Vertical Acceleration Tower (VAT) and recommend a basic dynamic vertical test exposure. Preliminary data will be provided to drive future research to develop appropriate occupant-based performance metrics, such as injury assessment reference values (IARVs) of supine occupants in litters. Longitudinal, lateral, and combined loading were out of scope for this research.

This space is intentionally blank.

Methods

Litter Configurations and ATD Selection

The Talon II 90C was selected for dynamic testing because it was deemed more vulnerable than the decontaminable litter due to its hinged litter pole construction. The Talon II 90C litters acquired for the APMS consisted of the following main components: two parallel bars, each equipped with two supporting feet (one near the head of the patient at the end of the pole and one near the foot end of the patent); two spreader bars between the poles attached near each support foot; webbing, spanning between the poles; and two integrated patient restraint straps (one near where the chest of the patient would be expected and one near the knees) (Figure 2).

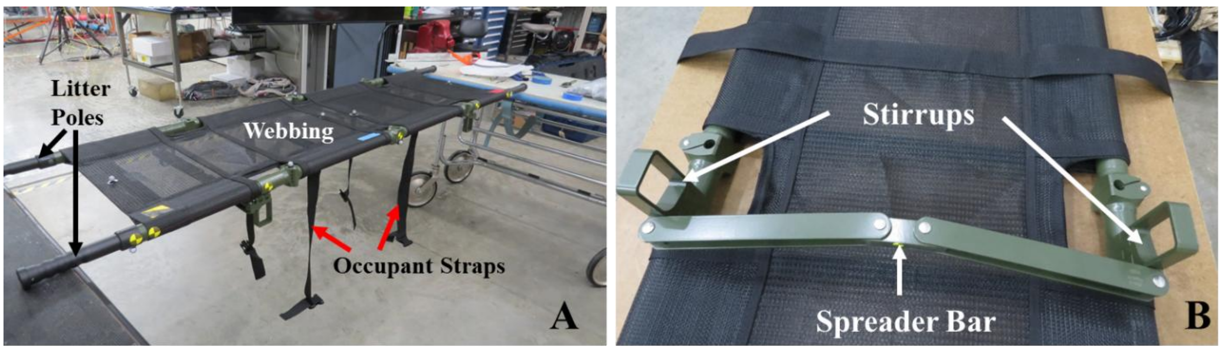

Figure 2. The Talon II 90C litters used for this study consisted of a webbing expanded between two litter poles (A). The bottom view of the litter shows the left and right stirrups and spreader bar (B).

The Pedestrian Pelvis variant of the standard Hybrid III 95th percentile male (HIII-95M-PED) (The Humanetics Group, Farmington Hills, MI) with standard legs was selected because its revised pelvis design allows the legs to rotate from a seated to a supine position. The litter was occupied by the 223.1 lb HIII-95M-PED to simulate a large patient loaded on the APMS under operational conditions. The ATD neck angle was adjusted to place the head in its most upright/vertical position to minimize the distance between the back of the head and the litter webbing when the ATD was placed on the litter in a supine position. Since the shoulder bracket rested on the litter poles, the ATD arms were disarticulated, and the shoulder brackets were removed to induce a more realistic representation where the litter webbing supported the chest during vertical loading.

Before the restraints were applied, the disarticulated arms were positioned along the sides of the ATD and supported by the litter poles. The ATD shoulder bolt holes were aligned with the first hinge of the litter pole on both sides to ensure consistent positioning. To prevent the "floating" arms from sliding out of the restraints, a strap was passed through the chest jacket of the ATD, connecting the arms together and reducing the probability of movement (Figure 3). The arms were positioned by the side of the ATD with the hands pressed against the simulated skin of the thigh. The ATD mid-sagittal plane was positioned along the litter left/right center line with the crown of the head at the edge of the litter webbing. The ATD legs were positioned straight, outstretched with the medial aspect of the ankles touching each other. The pelvis was then adjusted to allow only minimal rotation of the femur/hip joints. The positioning of the head, chest, pelvis, and feet of the ATD were confirmed by projecting a laser alignment line along the center line of the litter.

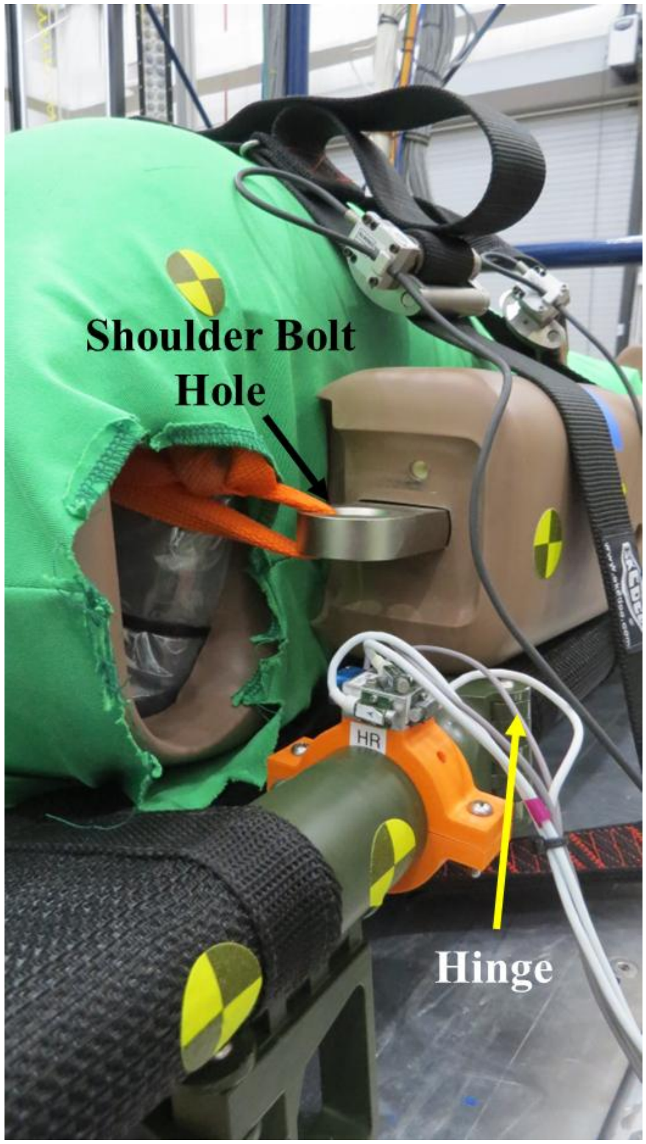

Figure 3. The arms were disarticulated at the shoulder to avoid artificial rigid contact of the ATD shoulder bracket with the litter poles. An orange strap was passed through the arm opening of the ATD chest jacket to tether the arms.

This space is intentionally blank.

The USAARLVAT was configured to accept floor-mounted and elevated APMS platforms (Figure 4). The floor-mounted APMS consisted of a simulated aircraft floor with track mounts used as anchor points to secure the litter and simulated patient to the simulated aircraft floor (Figure 4). Two integrated litter straps (blue) were used to secure the ATD to the litter, and three straps (green) with quick disconnect adapters (indicated by yellow ovals) were used to secure the APMS and patient to the simulated aircraft floor (Figure 5). Strap placements for the floor and elevated conditions were determined with the assistance of a retired U.S. Army flight medic and mimicked a real-world patient loading scenario as closely as possible.

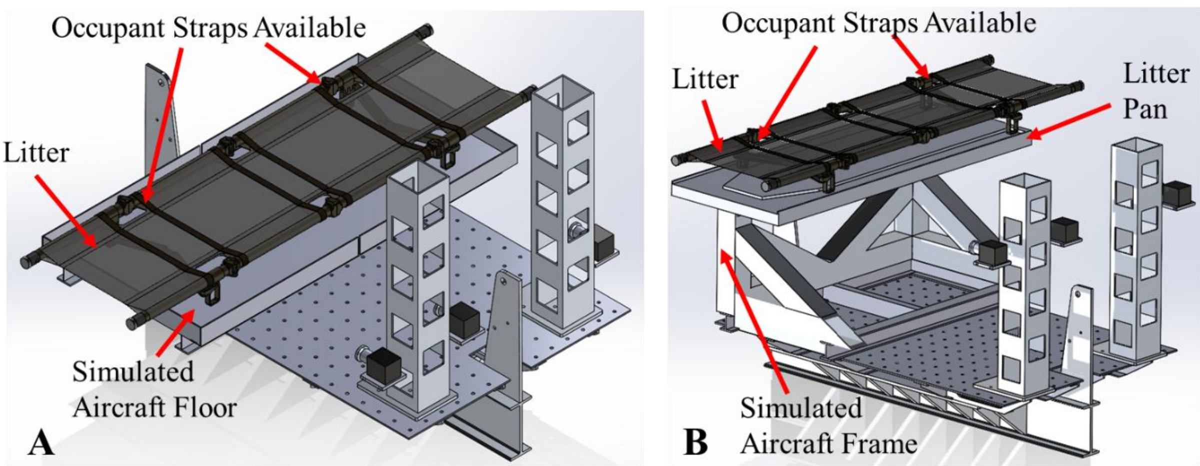

Figure 4. Floor-mounted (A) and elevated platform (B) APMS fixturing was designed for the VAT.

This space is intentionally blank.

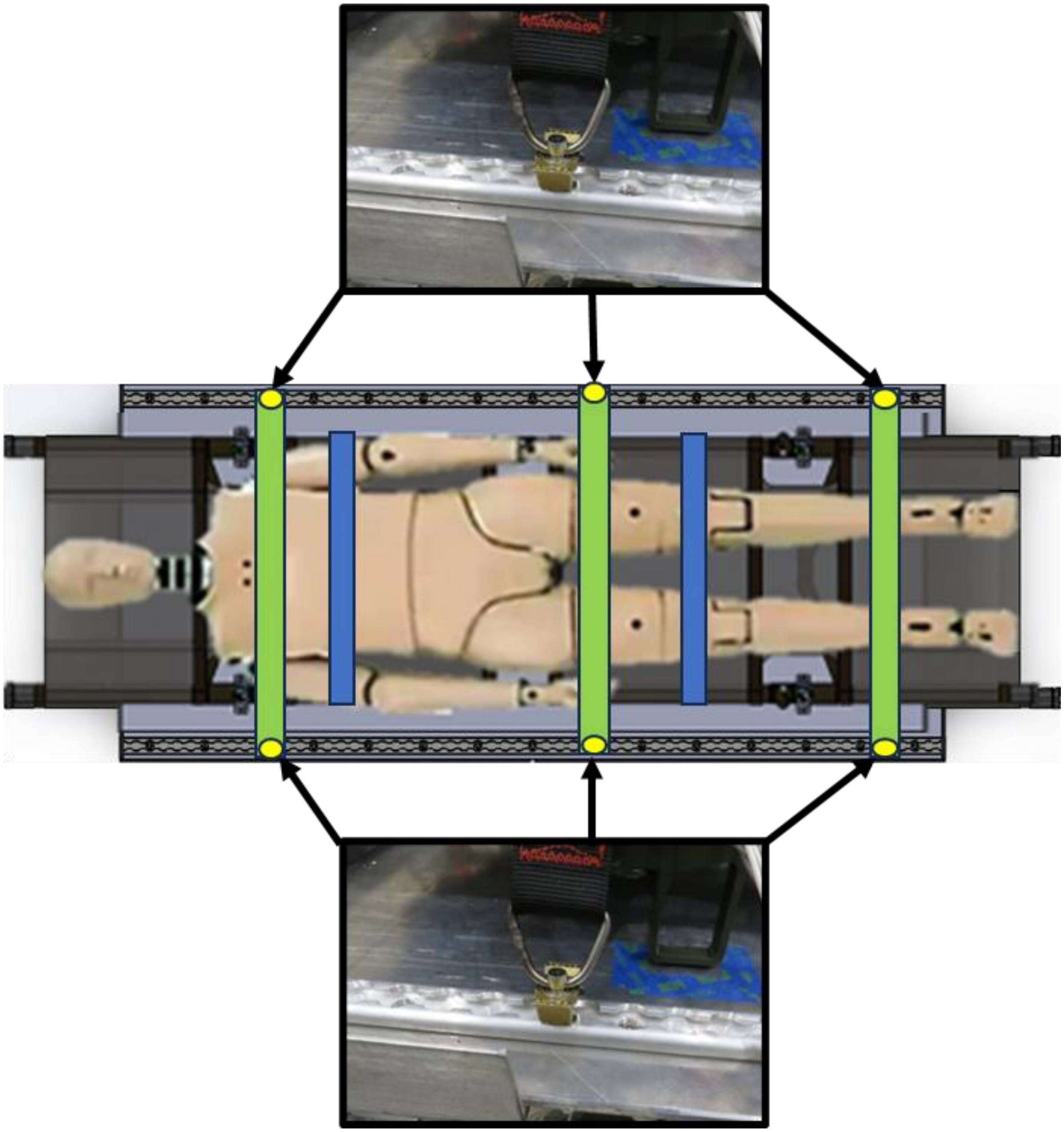

Figure 5. The floor-mounted APMS consisted of a litter with two integrated occupant straps (blue) securing the ATD to the litter and three straps (green) securing the APMS and patient to a track in the simulated aircraft floor with quick disconnect adapters (indicated by yellow ovals).

This space is intentionally blank.

Since it was not possible to replicate the full elevated mounting system without the use of an actual airframe (resulting in a prohibitive mass for the VAT), the test fixture consisted of only the pins, litter pan support, and compatible litter pan. Integrated Modular Medical Support System (IMMSS) pins were used to attach the litter pan support to the simulated airframe, which supported the elevated litter pan and litter (Figure 6). The design of the elevated APMS was different from the floor-mounted APMS—the elevated litter pan was shorter and did not have as many places to secure the patient and litter to the litter pan (Figure 7). Therefore, the ATD was secured to the litter on the elevated litter pan with three straps: two integrated straps (blue) like the floor-mounted APMS, and an extra strap (yellow) around the lower extremities and litter to prevent excessive flail during the test. Three straps (green) with quick disconnect adapters (indicated by yellow ovals) secured the APMS and ATD to the litter pan as shown in Figure 7.

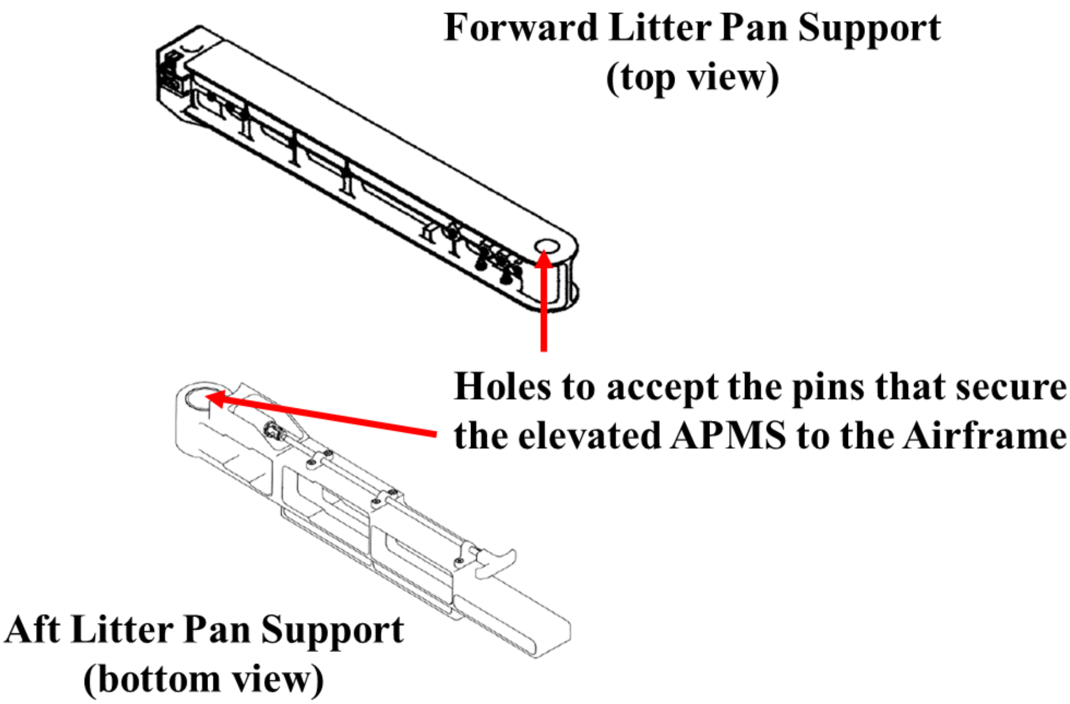

Figure 6. The elevated APMS components (not pictured in Figure 4) that connected to the simulated airframe to support the litter pan and litter.

This space is intentionally blank.

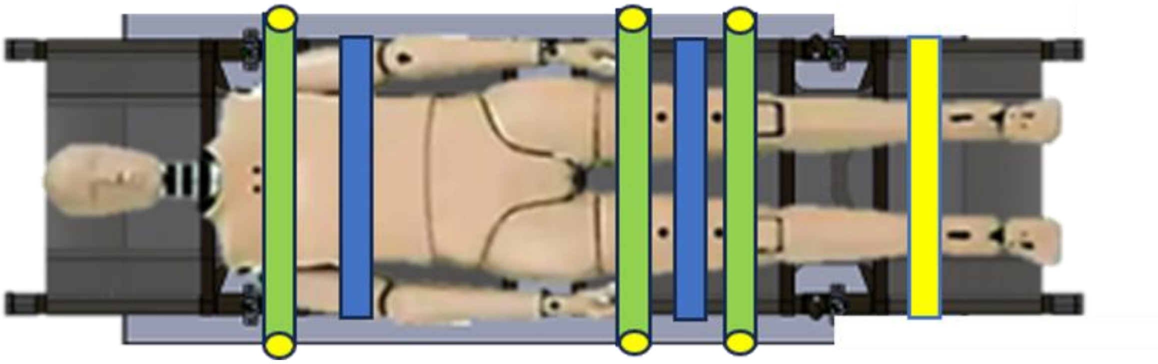

Figure 7. The elevated APMS configuration consisted of a litter with two integrated occupant straps (blue) that secured the ATD to the litter and three straps (green) with quick disconnect adapters (indicated by yellow ovals) that attached underneath the elevated litter pan to secure the litter and ATD. A third occupant strap (yellow) was added around the lower legs of the ATD and the litter to remain consistent with the floor-mounted APMS restraints and prevent the legs from flailing.

The ATD was secured in the supine position to each litter with patient restraint straps consistent with the current practice in the operational field (Department of the Army, 1991) (Figure 8). The pre-test tension of the restraints was determined by a retired flight medic. The retired flight medic loaded the ATD onto the litter as a patient would be loaded in theatre and tightened each strap three times for consistency. The pre-test tension range of the restraints was developed from the average of the three strap adjustments. Positioning of the ATD in the litter was documented using a FARO® ScanArm (Quantum model, FARO Technologies, Lake Mary, FL) and the impact test event was captured using high-speed video (HSV).

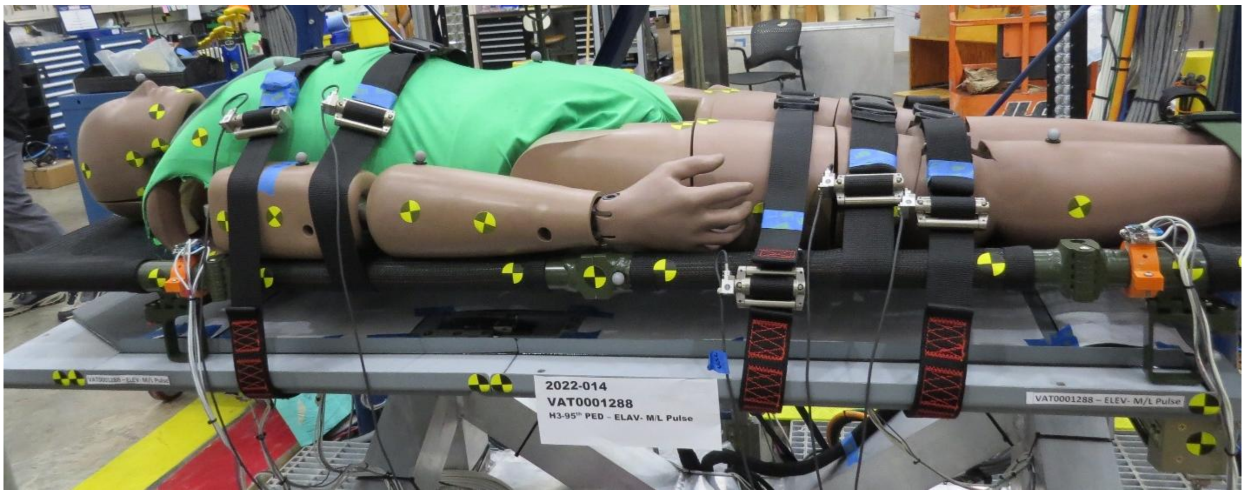

Figure 8. The ATD placed in the elevated configuration during both APMS configurations is shown.

Coordinate Systems

The coordinate system (CS) for the ATD and test fixtures are documented in Figure 9. The supine ATD CS was consistent with SAE J211-1 guidelines (SAE International, 2007). The global CS of the APMS was kept consistent with the conventional aircraft CS as per the ACSDG (Desjardins et al., 1989).

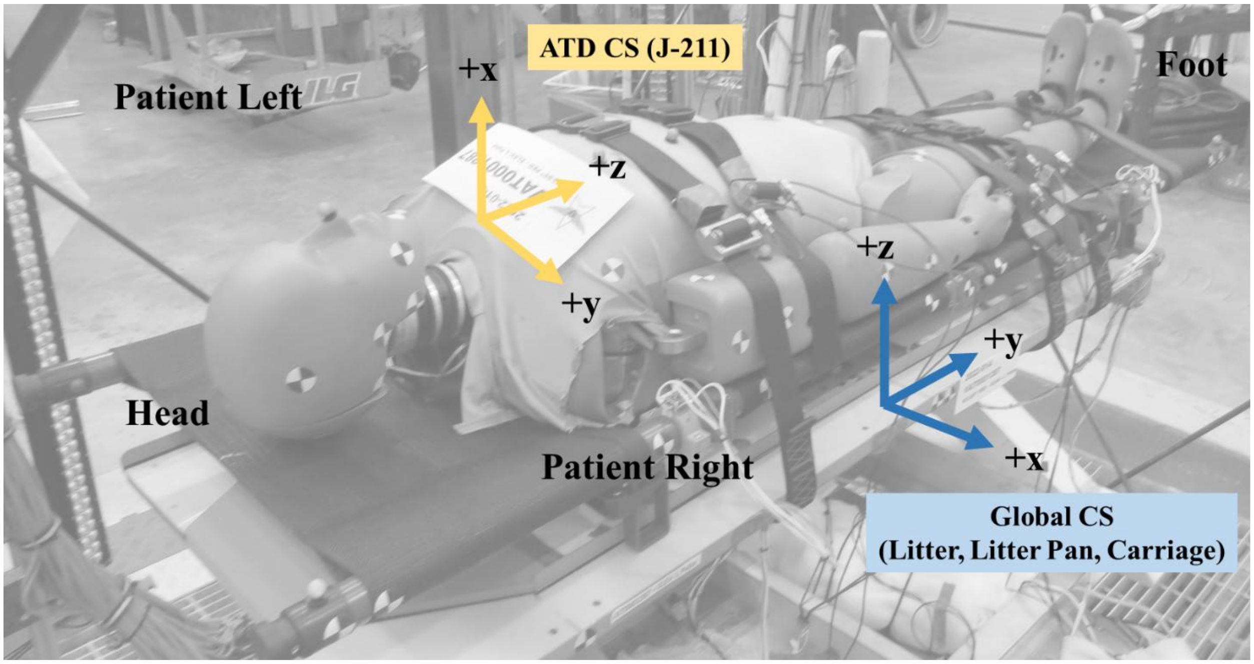

Figure 9. The CS of the ATD and the APMS were consistent with the 2007 version of the SAE J-211-1 guidelines and the ACSDG, respectively.

This space is intentionally blank.

Pulse Development

The HIII-95M-PED and APMS were exposed to two vertical accelerative test severities to assess the structural integrity of the APMS and response of the ATD during the dynamic event. Due to the severity of the 48 G dynamic test recommended by the ACSDG, an incremental approach was chosen. Although MIL-L-49511B (DoD, 1997) does not specify dynamic test requirements, a low dynamic performance level was calculated from its 1600 lb static load test for permanent deformation. A low severity dynamic exposure was calculated for this study by dividing the 1600 lb static load by an occupant mass of 223 lb (the HIII-95M-PED weight) (Equation 1). The resulting severity calculated was 7.2 G, which was rounded to 7 G due to the control limitations of the VAT. For a 7 G acceleration pulse, a velocity change of 25 ft/s was selected due to the stroke limit of the VAT. A medium severity dynamic exposure of 20 G was selected as this acceleration level approximated the seat pan response threshold specified in MIL-S-58095A for crashworthy pilot seats when the seating system is exposed to a vertical 46 G triangular acceleration pulse. The 25 ft/s velocity change was applied to this test condition to maintain consistent energy levels with the low severity dynamic pulse. For comparative purposes, a 25 ft/s velocity change has 35.4% of the energy as the MIL-S-58095A test requirement of 42 ft/s for pilot seats,

$$a = \frac{F}{m} \tag{1}$$

$$a = \frac{1600}{223} = 7.2\text{ G}$$

This space is intentionally blank.

Instrumentation

The VAT carriage was instrumented with accelerometers and a thrust load cell to measure the input pulses. Additional accelerometers were mounted to the litter (Figure 10) and various structural components supporting the elevated APMS (Figure 11) to examine how the components reacted to the pulse. The ATD acceleration in the head, chest, and pelvis and force/moment loads in the femur were recorded.

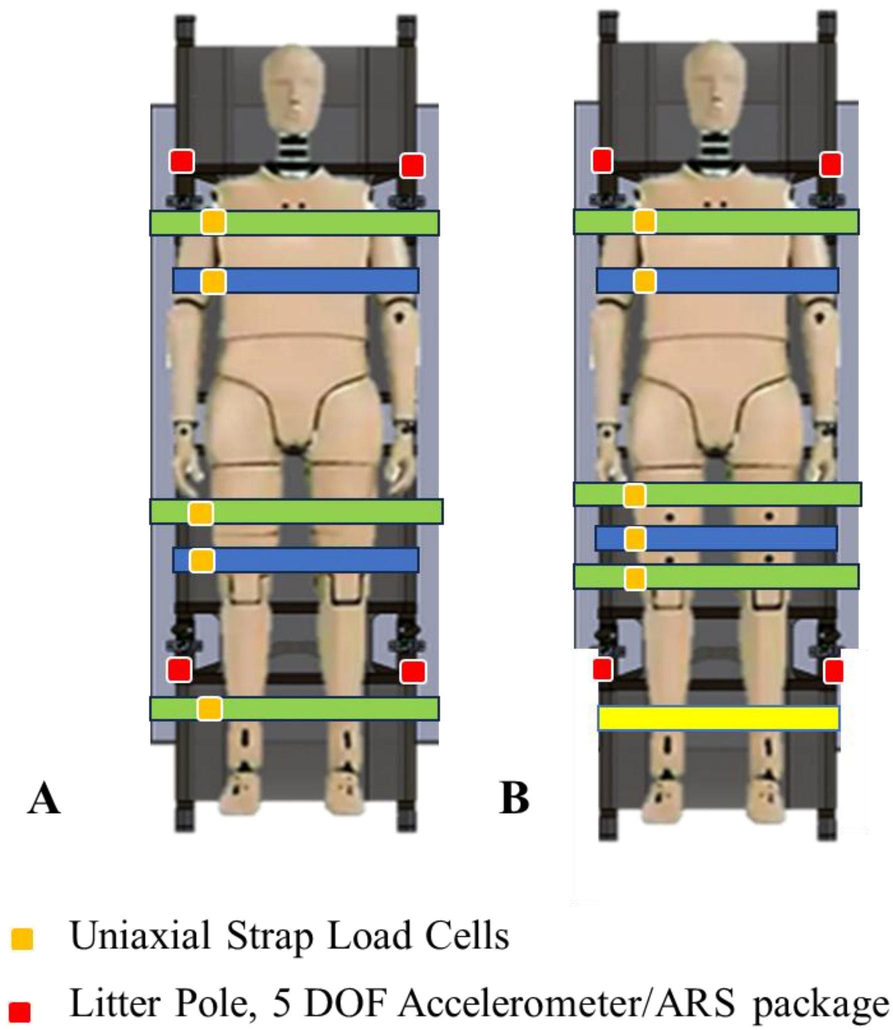

Figure 10. The litter was instrumented with four five-degree-of-freedom (5DOF) accelerometers and an angular rate sensor package (red). The straps were instrumented with restraint load cells (orange). Blue straps secured the ATD to the litter and green straps secured the ATD and litter into the APMS. The floor-mounted configuration (A) had five straps (blue and green). The elevated configuration (B) also had five straps (blue and green) but, due to geometry, an extra un-instrumented strap (yellow) was used to prevent lower extremity flail.

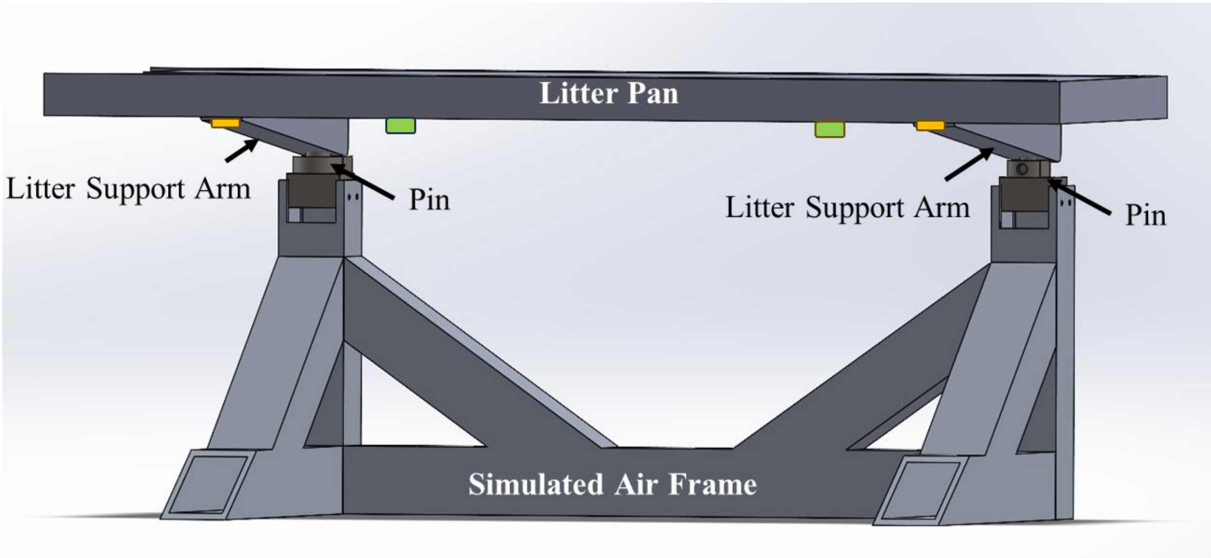

Figure 11. The elevated APMS was instrumented with two accelerometers centered on the bottom of the litter pan (green) under the chest and lower extremities of the ATD. One accelerometer was also mounted to the end of each litter support arm (yellow).

Data Collection

Each targeted severity pulse (7 and 20 G) was conducted three times each for the floor-mounted and elevated APMS configurations for a total of 12 tests. All ATD-related sensor data—force, moment, angular rate, and acceleration—were collected at a rate of 200,000 samples per second (sps). Carriage pulse data, including accelerations and load cell forces, were also collected at 200,000 sps. The acceleration events and overall ATD responses were documented using multiple, digital, HSV cameras. The HSV images were recorded at 2,000 frames per second. All sensor data acquisition and HSV documentation were synchronized using a common trigger signal initiated by carriage motion. Pre- and post-test photographic images were taken for each test. Data was collected and filtered according to SAE J211-1 guidelines (SAE International, 2007). Additional steps were taken to capture contact of the ATD with the simulated aircraft floor and litter pan structures. These measures included graphite paper lined under the litter to identify ATD contact locations and a dyed oil coating on the spreader bars to mark structural contact. All structural elements were visually inspected and deformation was documented with scans using an Artec Leo (Artec 3D, Luxembourg) and photographs. The webbing and straps were inspected after each test. Each litter was collapsed and reopened after testing to confirm functionality.

This space is intentionally blank.

Results

Floor-Mounted APMS

Time traces of the carriage accelerations for the floor-mounted APMS at each targeted pulse are shown in Figure 12. It was noted that the targeted 20 G pulse resulted in a 23 G pulse. Results reported for the higher pulse will be reported as 23 G tests.

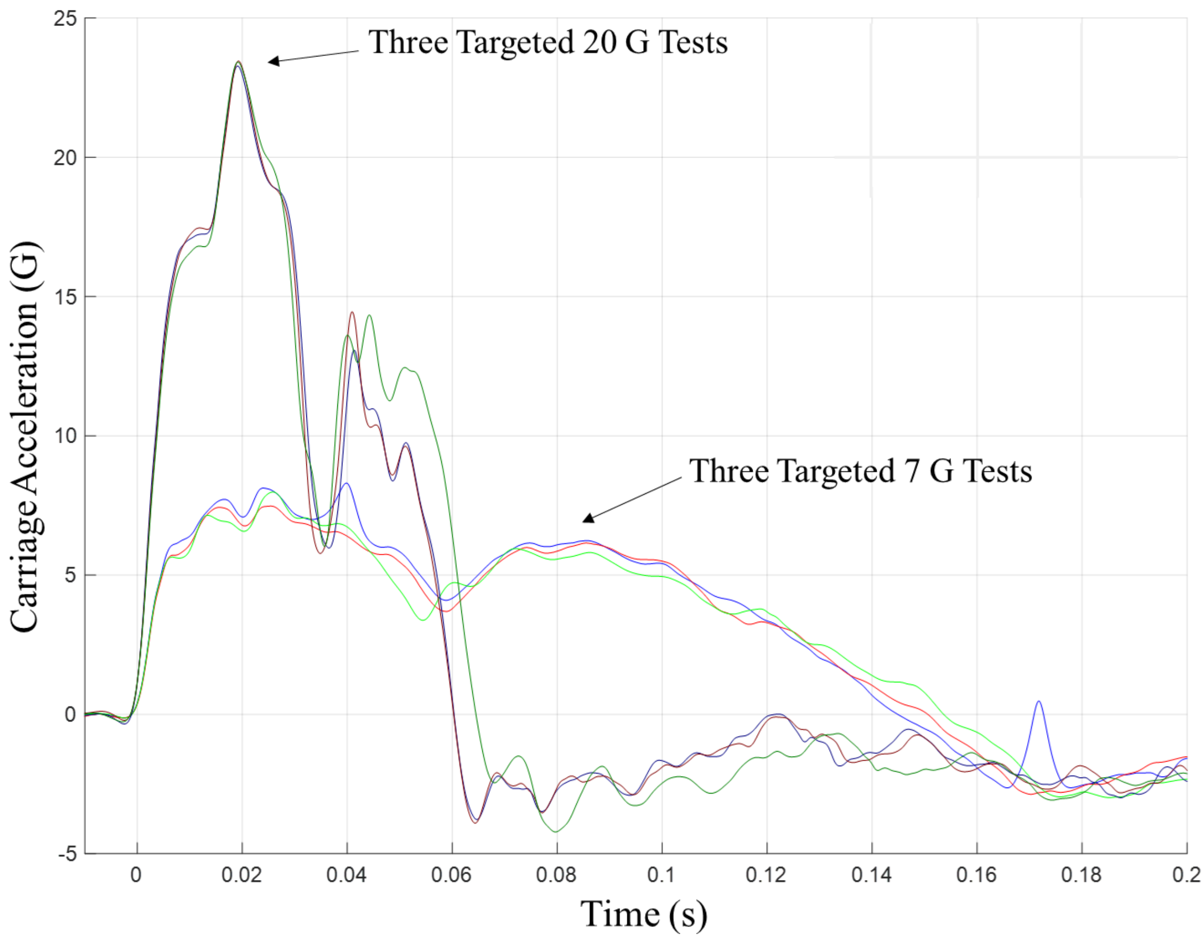

Figure 12. The floor-mounted APMS was exposed to targeted 7 G and 23 G pulses. Carriage acceleration and time were recorded for the six tests.

This space is intentionally blank.

Acceleration versus time data of the carriage, ATD sensors, and litter poles for the floor-mounted APMS configuration were plotted. This demonstrates the response times of the components as the pulse progresses through the load path. Figures 13 and 14 show one representative during the targeted 7 G and 23 G pulse, respectively. The acceleration data indicated that the ATD chest and pelvis contacted the simulated aircraft floor. It was noted in both floor pulses, all four litter pole mounted accelerometer data tracked the carriage pulse well with only a small initial delay (indicated by the red arrow) and increased overall oscillation.

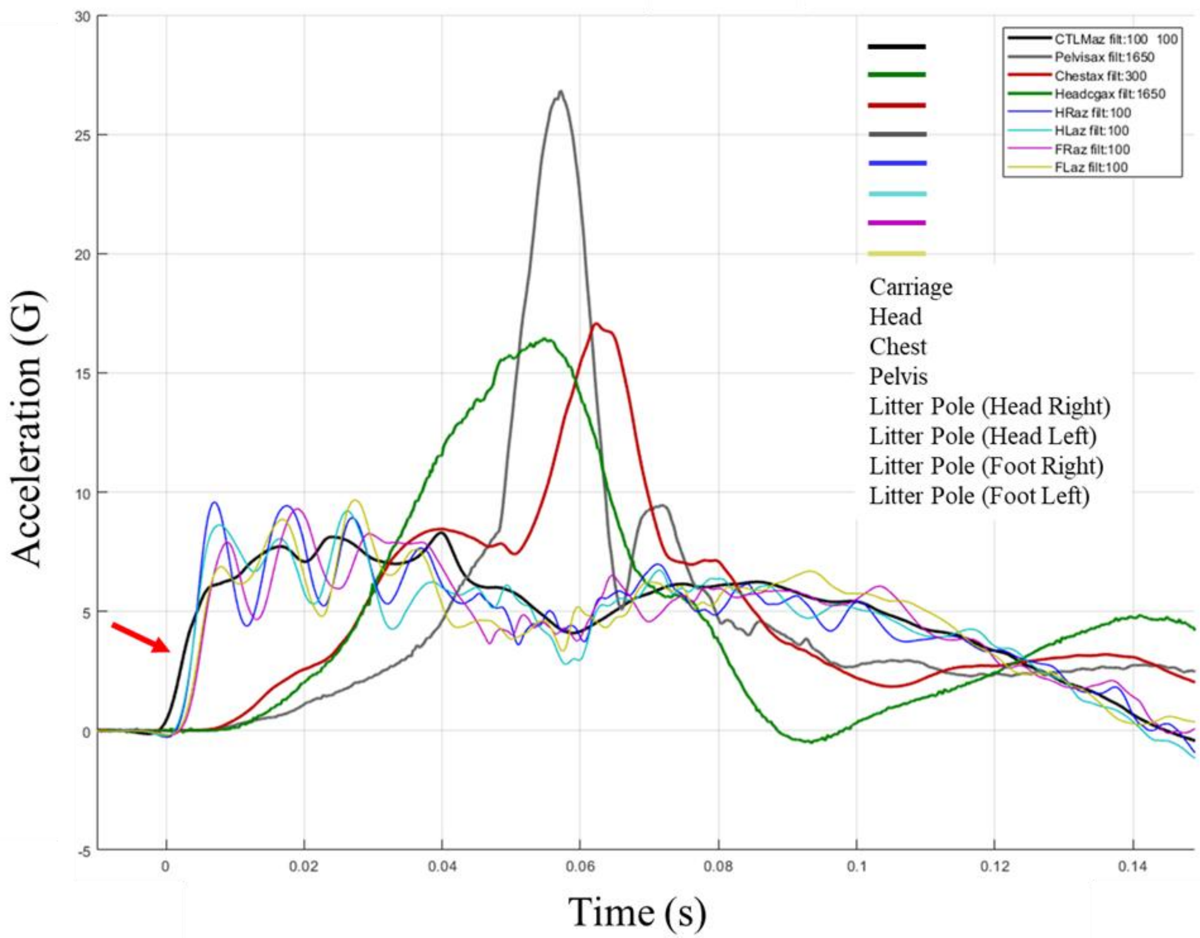

Figure 13. Carriage, ATD head, chest, and pelvis, and the four litter pole acceleration versus time data from one of the 7 G pulses for the floor-mounted APMS test were plotted. A small initial delay between the carriage acceleration and the litter poles, indicated by the red arrow, was noted.

This space is intentionally blank.

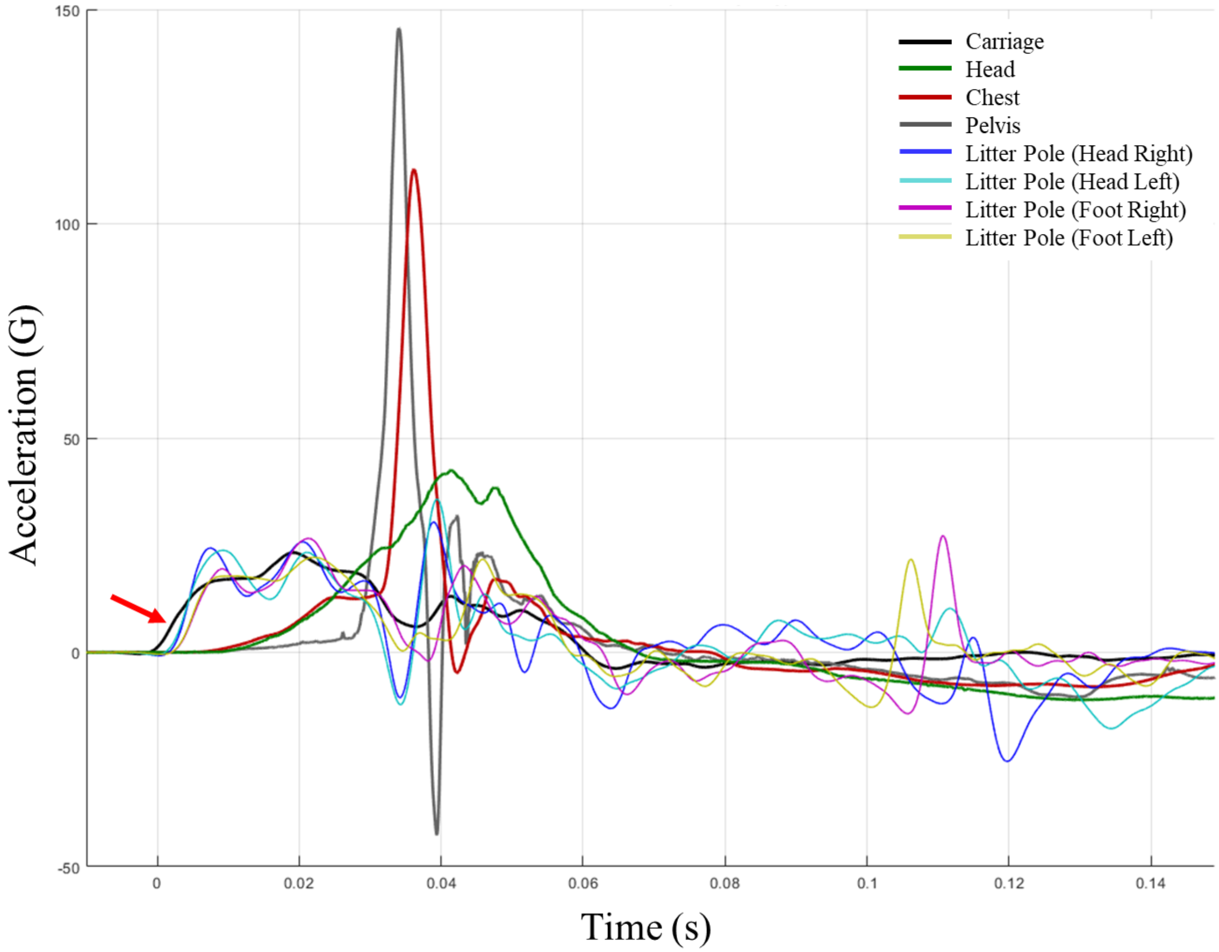

Figure 14. Carriage, ATD head, chest, and pelvis, and the four litter pole acceleration versus time data from one of the 23 G pulses for the floor-mounted APMS test were plotted. A small initial delay between the carriage acceleration and the litter poles, indicated by the red arrow, was noted.

This space is intentionally blank.

Force and moment in the *x-, y-,* and *z-* direction (F_x, F_y, F_z, M_x, M_y, and M_z) versus time data of the femur load cells for the floor-mounted APMS configuration were plotted. Figures 15 and 16 show one representative test during the targeted 7 G and 20 G pulse, respectively. It was noted that a large M_y in the right and left femur saturated beyond the capacity of the sensor during the 23 G pulse.

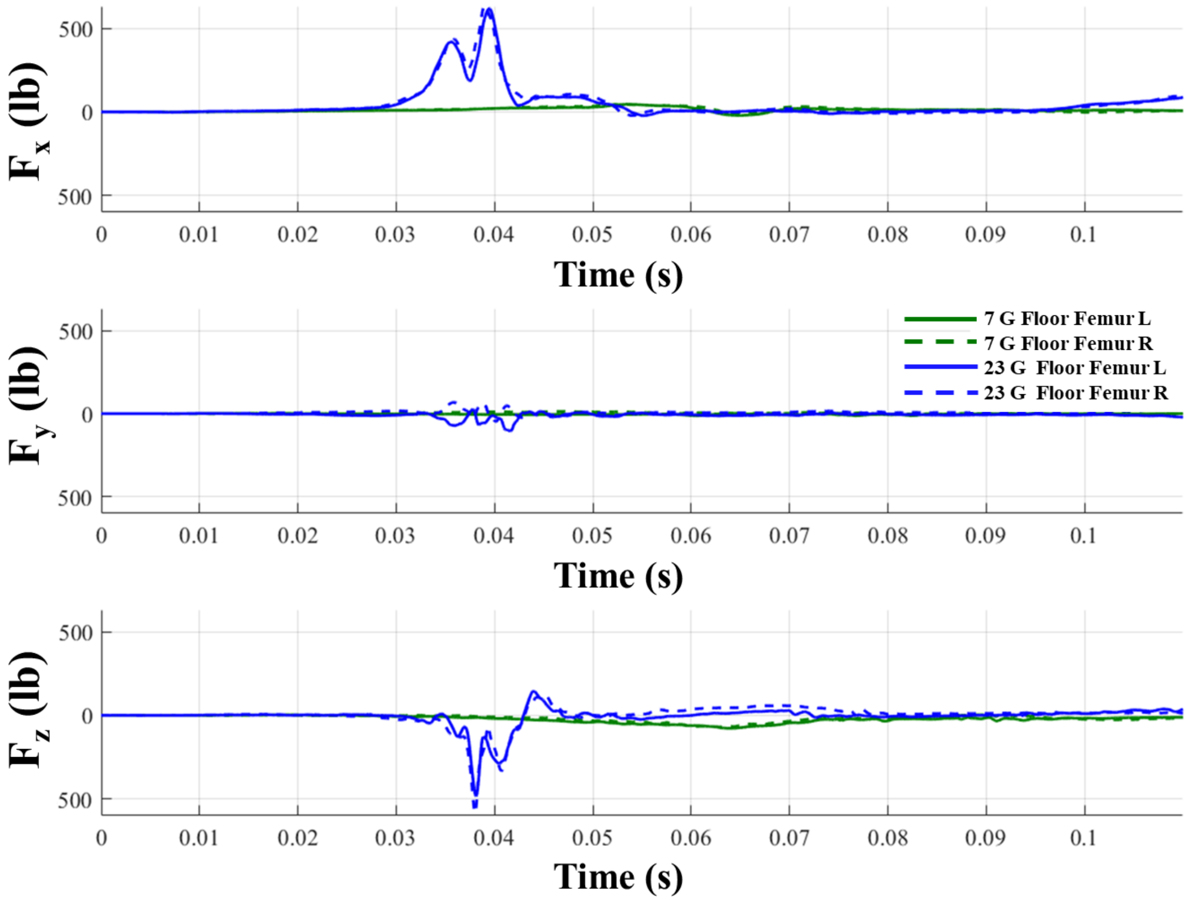

Figure 15. Forces in the *x*-, *y*-, and *z*- direction versus time data from one of the 7 G and 23 G pulses for the floor-mounted APMS test was plotted.

This space is intentionally blank.

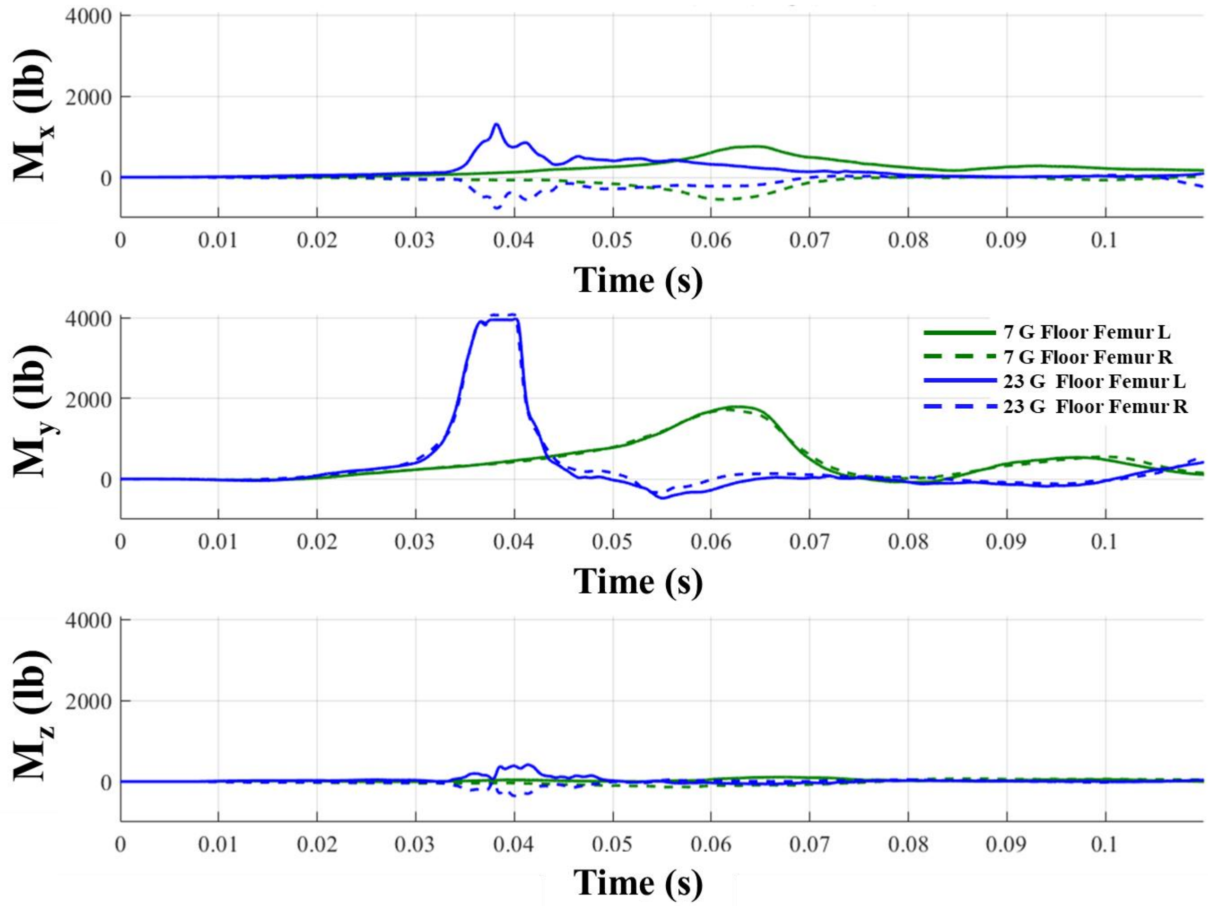

Figure 16. Moments in the *x*-, *y*-, and *z*- direction versus time data from one of the 7 G and 23 G pulses for the floor-mounted APMS test was plotted.

This space is intentionally blank.

The sensor data from each of the three pulse tests were averaged. Average peak accelerations of the ATD head, chest, and pelvis, peak F_x and M_y for the femur load cells in the floor-mounted APMS configuration were documented in Tables 1 and 2. Over 160 percent (%) changes in Peak A_x were noted between the 7 G and 23 G pulses. Sensor data for the three individual tests can be found in the Appendix Table A1 and A2.

Table 1. Average Peak ATD Accelerations for the Head, Chest, and Pelvis in the *x*-Axis Direction for the Floor-Mounted APMS Configuration

	Peak A*x* (G)					
Pulse	**Head**	**% Change**	**Chest**	**% Change**	**Pelvis**	**% Change**
7 G	15.8	161.3%	18.3	590.3%	29.5	441.0%
23 G	41.4		126.3		159.6	

Table 2. Average Peak ATD Right and Left Femur Load Cell Force in the *x*-Axis and Moment in the *y*-Axis Directions for the Floor-Mounted APMS Configuration

	Peak F_x (lb)				**Peak M_y (in-lb)**			
Pulse	**Right Femur**	**% Change**	**Left Femur**	**% Change**	**Right Femur**	**% Change**	**Left Femur**	**% Change**
7 G	72.4	857.9%	60.5	1006.0%	1538.4	165.5%	1739.8	130.6%
23 G	693.9		668.7		4084.2†		4011.4†	

†Channel saturated beyond capacity of sensor.

Before and after each test, the litter poles were supported at the ends and deformation of the litter webbing was documented with Artec Leo (Artec 3D, Luxembourg) scans. Figure 17A shows the deformation of the litter from beneath. After the 23 G pulse, some webbing deformation was noted for the floor-mounted APMS (Figure 17A) as indicated by the color scale in the legend. There was also minimal deformation in the hinge of the litter poles as shown in the side view (Figure 17B).

This space is intentionally blank.

Review of the HSV data revealed the ATD contacted the simulated aircraft floor for all floor-mounted tests. Figure 15 shows isolated frames of the two camera views focused on the head/chest (left) and pelvis/lower extremities (right) at time-zero (A), during contact (B), and during rebound (C) of the 23 G pulse. The stirrups of the litter poles leave the floor, as seen in Figure 15C, and re-contact the floor several times as the event progresses. There were no elongations and/or abrasions to the restraint webbing noted.

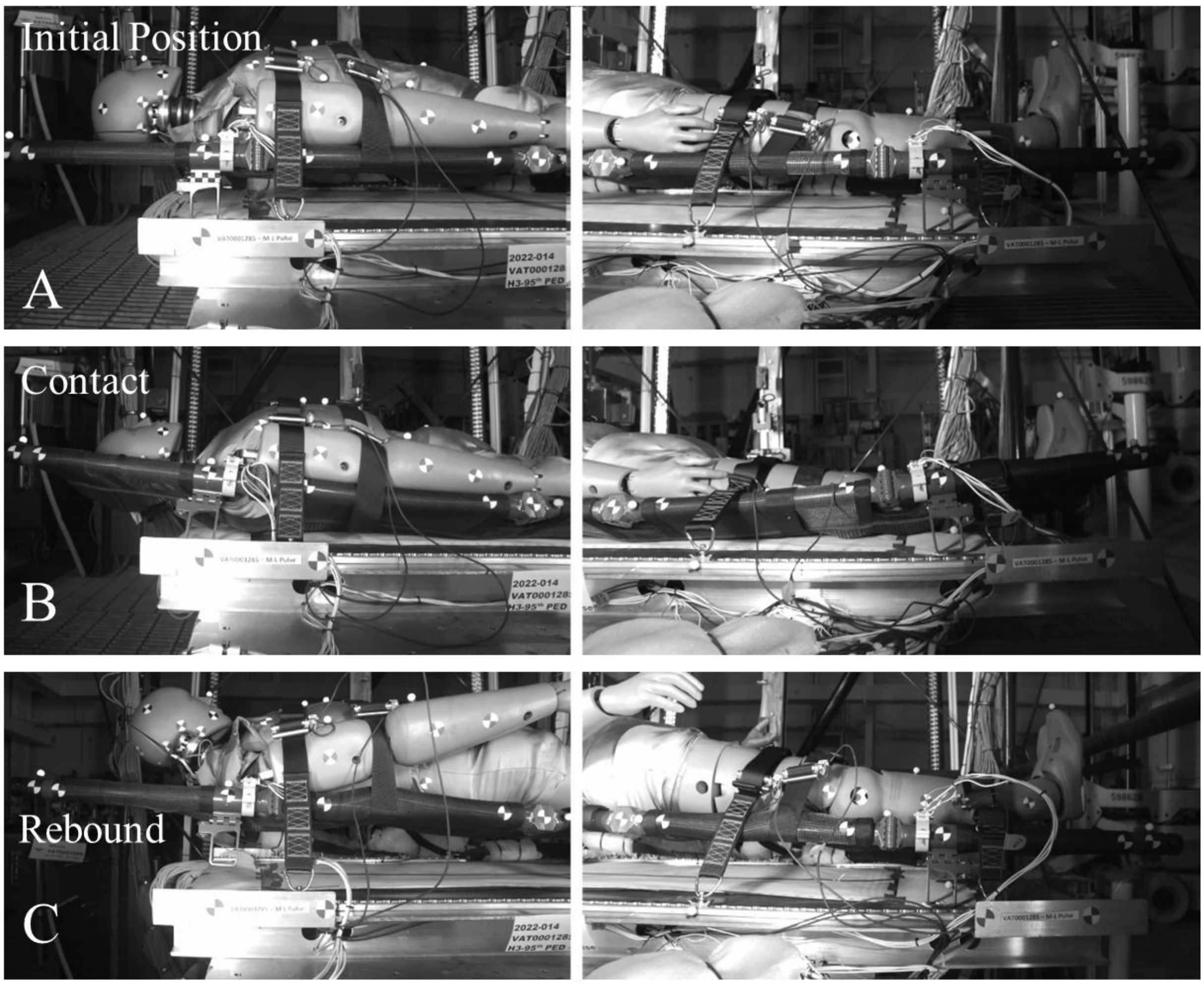

Figure 17. Views from the two cameras centered on the head/chest and lower extremities were combined to present a full-body image of the 23 G pulse. A time-zero frame (A), a frame where contact was observed (B), and a frame showing the rebound of the ATD (C) were selected from the HSV data for the floor-mounted APMS.

This space is intentionally blank.

The graphite paper that lined the surface of the simulated aircraft floor beneath the ATD and litter, confirmed contact for the chest, pelvis, and knees in all tests. Figure 16 shows the chest, pelvis, and knees contacted the simulated aircraft floor during the 23 G pulse. The head did not contact the simulated aircraft floor, but both spreader bars under the litter did make contact.

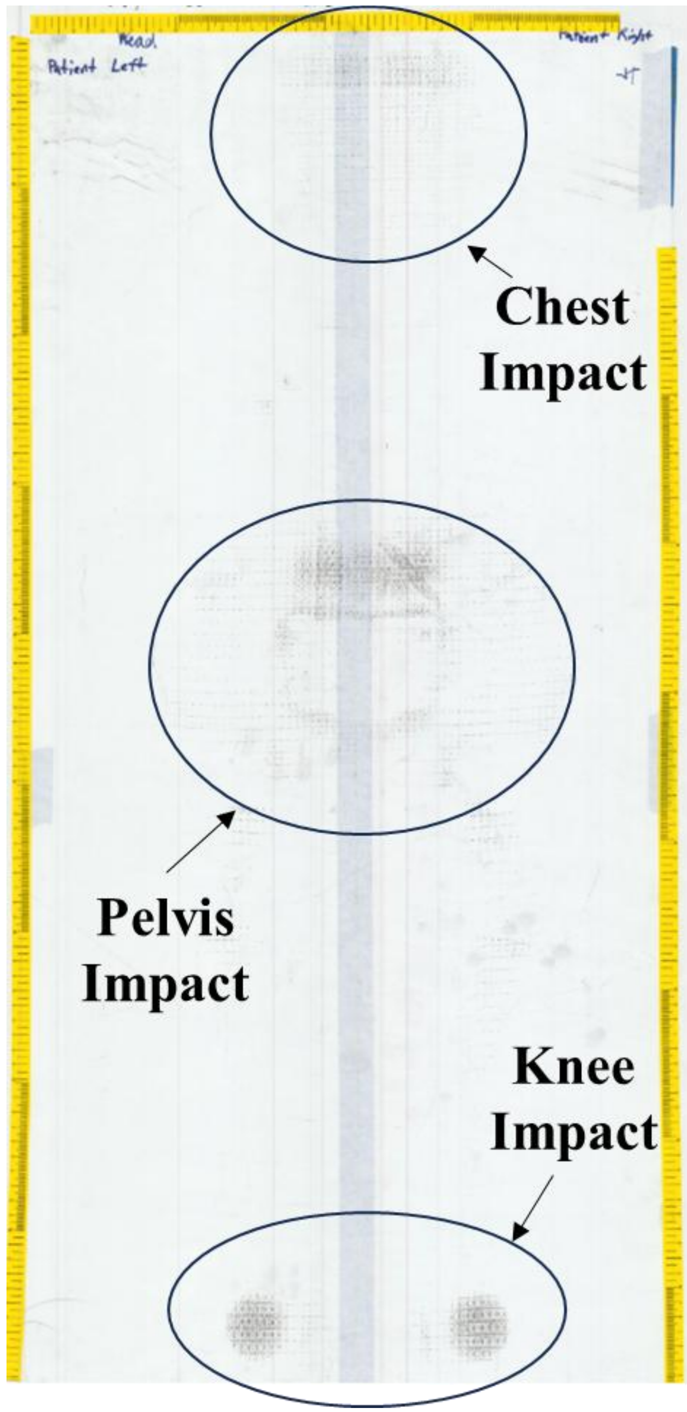

Figure 18. The ATD impacted the simulated aircraft floor during all pulses (imprint after one of the 23 G pulses is shown).

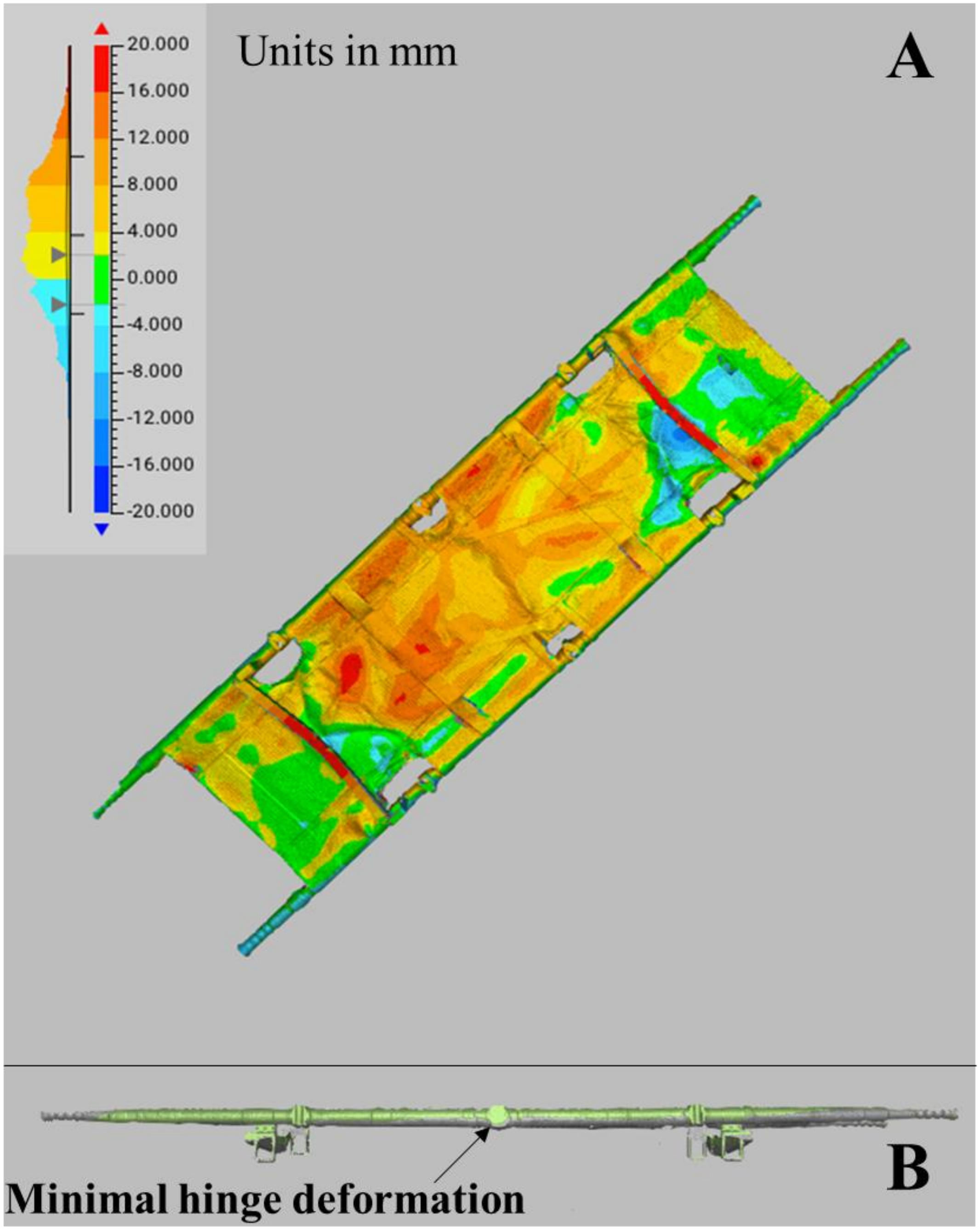

Figure 19. Bottom view (A) and side view (B) scans of the litter were taken of the floor-mounted APMS litter bottom to document webbing and component deformation after one of the 23 G pulses. Units of deformation in the legend are in millimeters.

Photos of the floor-mounted APMS spreader bars were taken from the head and foot ends of the litter for comparison before and after testing (Figure 18). The post-test inspection noted deformations in the spreader bars at the head and foot for all tests. The spreader bars in Figure 18C and D are closer to the simulated aircraft floor, indicating more deformation after the 23 G pulse. There was also splaying of the stirrups laterally (left and right of the patient). Although the spreader bars deformed, the litter could be collapsed and folded, and then re-opened and locked.

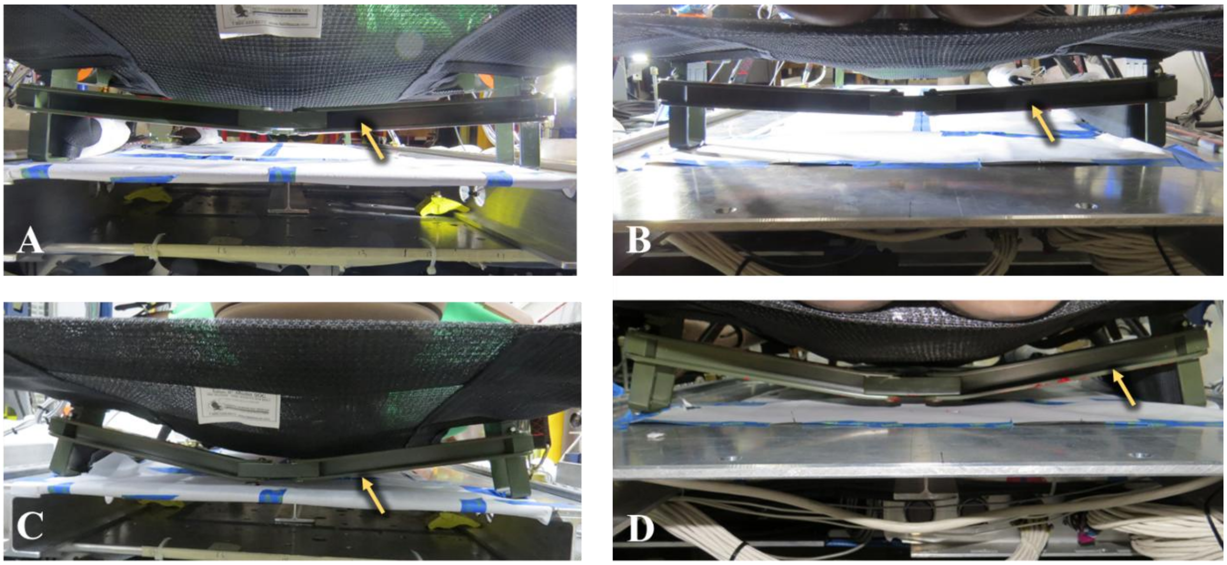

Figure 20. Pre-test photographs show the intact floor-mounted APMS spreader bars (yellow arrows) of the head (A) and foot (B). Deformation of the head (C) and foot (D) spreader bars (yellow arrows) after one of the 23 G pulses were noted post-test.

This space is intentionally blank.

Elevated APMS

The carriage accelerations of the elevated APMS at each targeted pulse are shown in Figure 19. It was noted that the targeted 20 G pulse resulted in a 23 G pulse. Results reported for the higher pulse will be reported as 23 G tests.

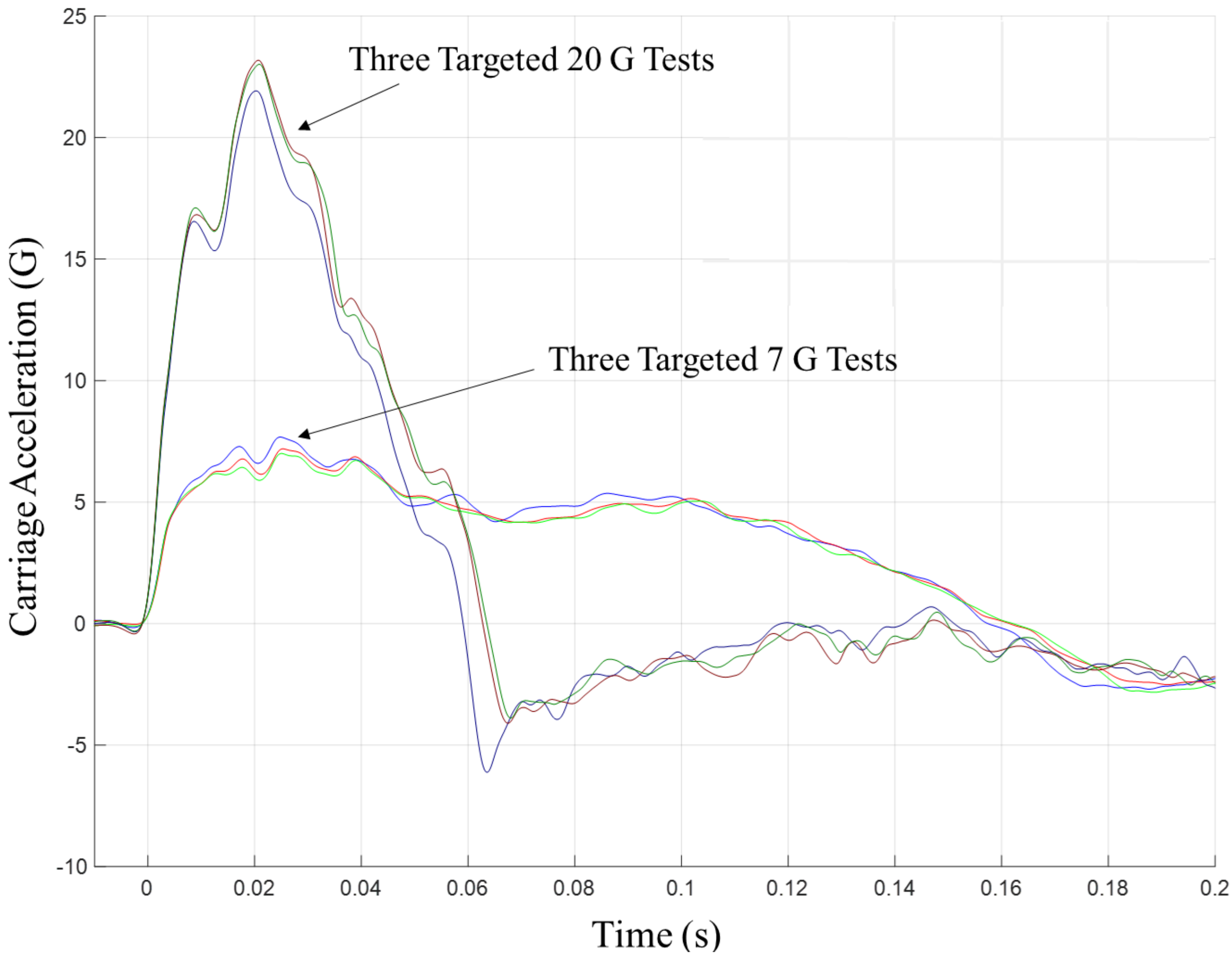

Figure 21. The elevated APMS was exposed to targeted 7 G and 23 G pulses.

This space is intentionally blank.

Acceleration versus time data of the carriage, ATD sensors, and litter poles for the elevated APMS configuration were plotted. This demonstrates the response times of the components as the pulse progresses through the load path. Figures 20 and 21 show one representative test of ATD sensors during the 7 G and 23 G pulse, respectively. The acceleration data indicated that the ATD chest and pelvis contacted the elevated litter pan. It was noted in both elevated pulses, all four litter pole mounted accelerometer data tracked the carriage pulse well with an initial delay (indicated by the red arrow) and some increased oscillation. Further, it was noted that the initial accelerometer data delay was smaller for the litter poles nearest the supporting simulated airframe (patient left) than the litter poles and litter support arm furthest away (patient right). Since the litter support arm acceleration data were similar to the patient right litter pole acceleration data, they are not included in the plots for simplicity.

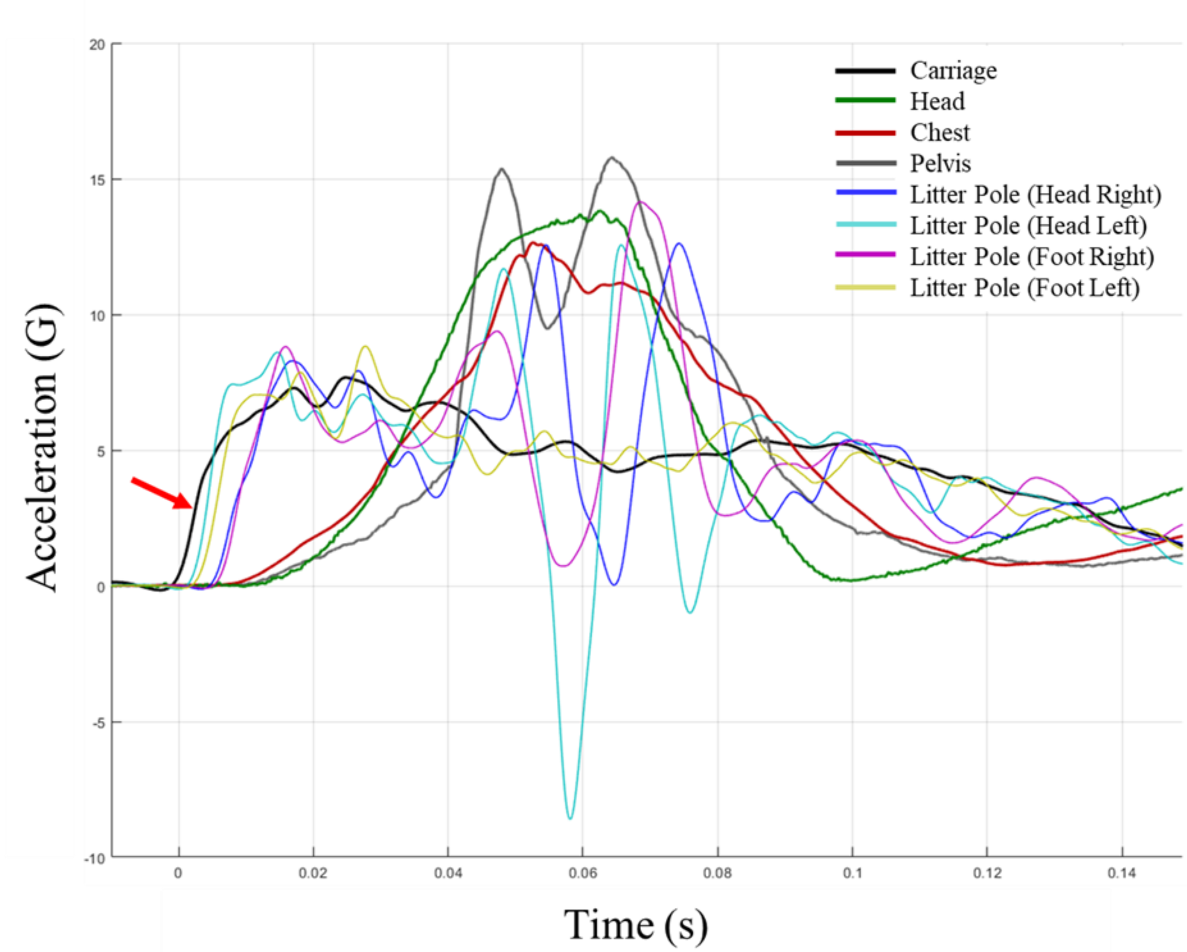

Figure 22. Carriage, ATD head, chest, and pelvis, and the four litter pole accelerations versus time data from one of the 7 G pulses for the elevated APMS were plotted. It was noted that the initial accelerometer data delay was smaller for the litter poles nearest the supporting simulated airframe (patient left) than the litter poles furthest away (patient right).

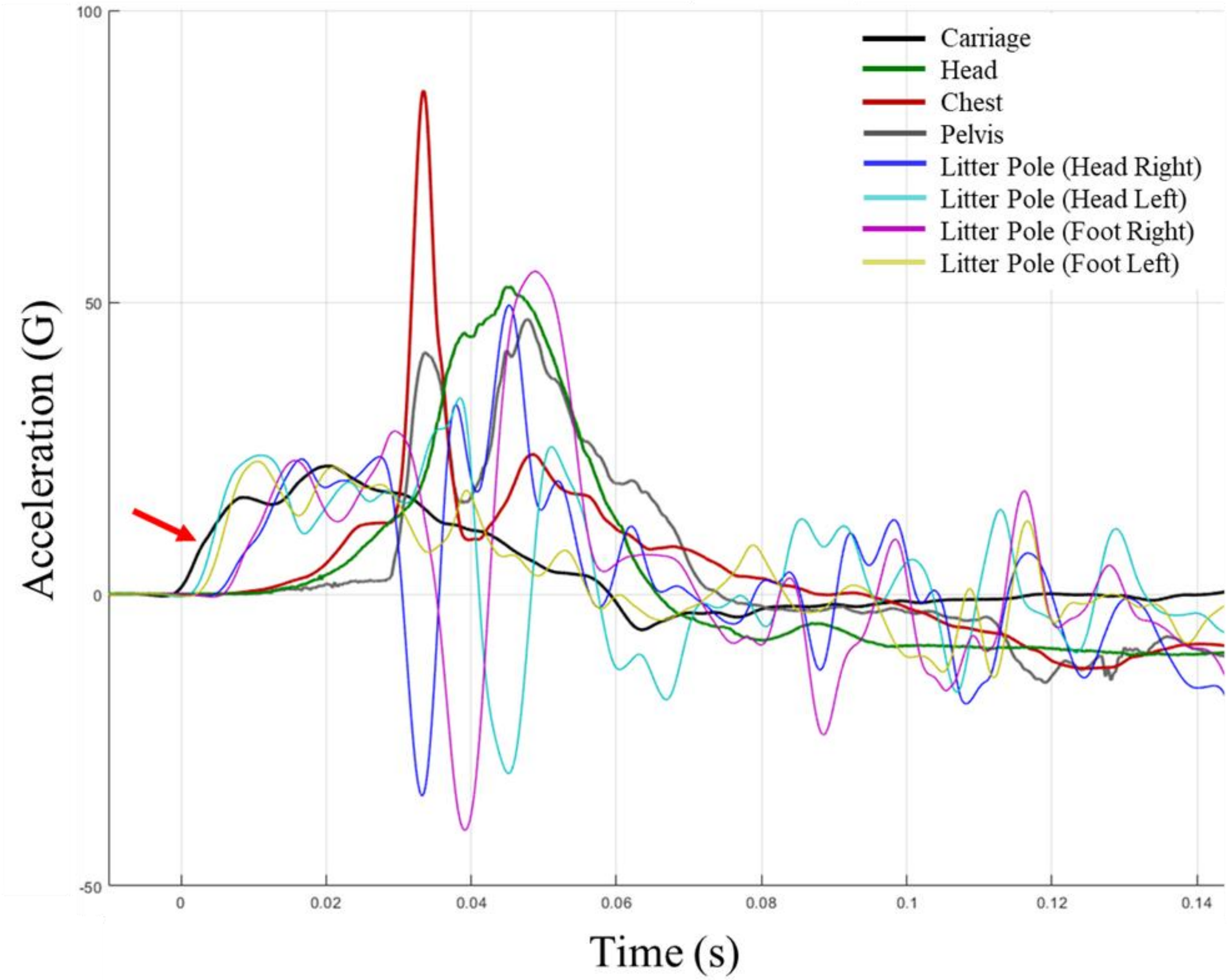

Figure 23. Carriage, ATD head, chest, and pelvis, and the four litter pole accelerations versus time data from one of the 23 G pulses for the elevated APMS were plotted. There was an initial accelerometer data delay, indicated by the red arrow, that was smaller for the litter poles nearest the supporting simulated airframe (patient left) than the litter poles furthest away (patient right).

This space is intentionally blank.

Force and moment (F_x, F_y, F_z, M_x, M_y, and M_z) versus time of the femur load cells for the elevated APMS configuration were plotted. Figures 24 and 25 show one representative test during the 7 G and 23 G pulse, respectively. A double peak was noted in the F_x and M_y sensor data. Additionally, a failure occurred in the M_z sensor in the 23 G elevated right femur.

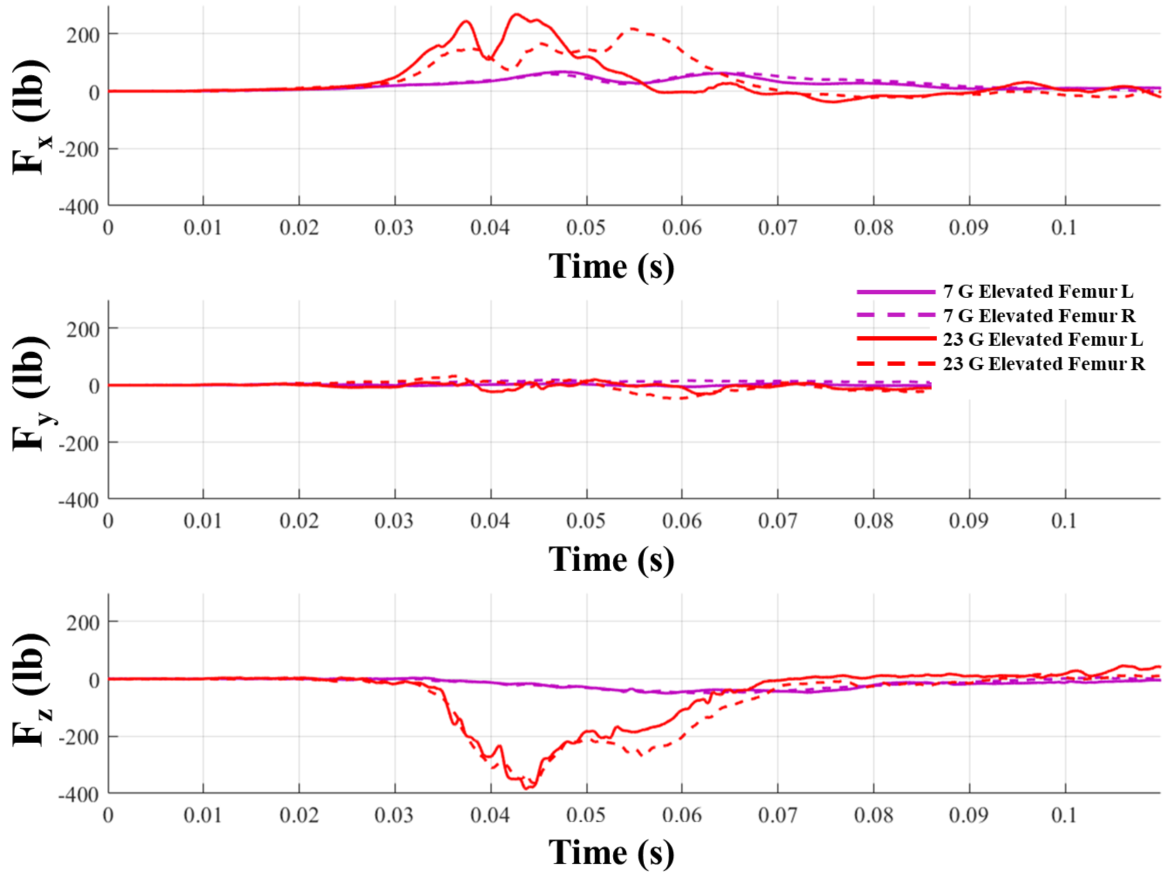

Figure 24. Force in the *x-, y-*, and *z-* direction versus time data from one of the 7 G and 23 G pulses for the elevated APMS test were plotted.

This space is intentionally blank.

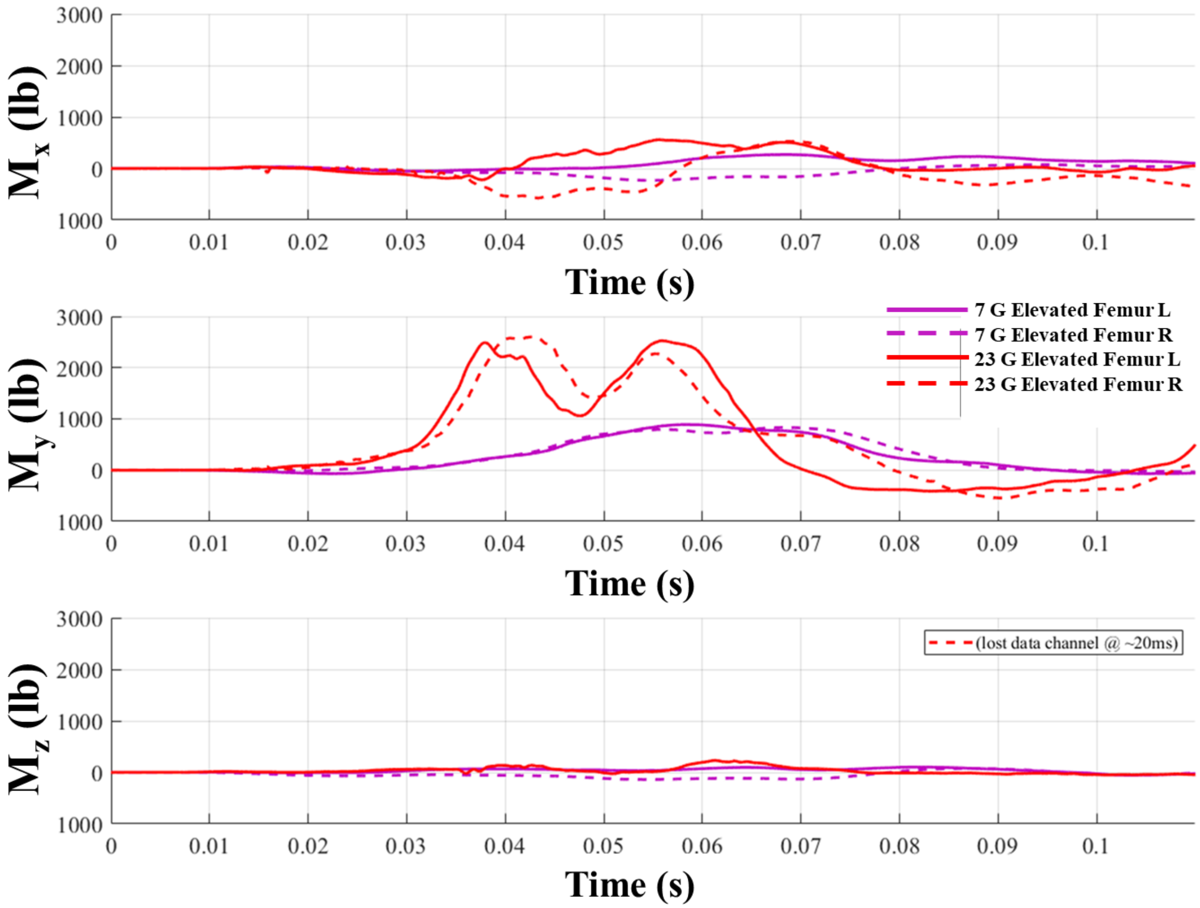

Figure 25. Moment in the *x-, y-*, and *z-* direction versus time data from one of the 7 G and 23 G pulses for the elevated APMS test were plotted.

Additionally, the sensor data from each of the three pulse tests were averaged. Average peak accelerations of the ATD head, chest, and pelvis and the peak F_x and M_y for the femur load cells were documented in the elevated APMS configuration in Tables 3 and 4. Over 190% changes were noted between the 7 G and 23 G pulses for all sensors reviewed. Sensor data for the three individual tests can be found in the Appendix Table A3 and A4.

Table 3. Average Peak ATD Accelerations for the Head, Chest, and Pelvis in the *x*-Axis Direction for the Elevated APMS Configuration

Pulse	Peak A*x* (G)					
	Head	**% Change**	**Chest**	**% Change**	**Pelvis**	**% Change**
7 G	13.3	338.5%	12.7	669.9%	15.7	192.1%
23 G	58.5		98.0		45.8	

Table 4. Average Peak ATD Right and Left Femur Load Cell Force in the *x*-Axis and Moment in the *y*-Axis Directions for the Elevated APMS Configuration

Pulse	Peak F*x* (lb)				Peak M*y* (in-lb)			
	Right Femur	**% Change**	**Left Femur**	**% Change**	**Right Femur**	**% Change**	**Left Femur**	**% Change**
7 G	61.2	304.6%	59.5	340.6%	769.8	255.8%	866.0	196.9%
23 G	247.5		262.2		2738.9		2571.2	

Before and after each test, the litter poles were supported at the ends and deformation of the litter webbing was documented with Artec Leo (Artec 3D, Luxembourg) scans. Figure 24A shows the deformation of the litter from beneath. After the 23 G pulse some webbing deformation was noted (Figure 24A) as indicated by the color scale in the legend; however, the hinges of the litter poles permanently deformed approximately 52.7 millimeters (mm) (Figure 24B).

This space is intentionally blank.

Contact and rebound of the ATD with the litter pan were observed in all tests when HSV data were reviewed (Figure 22). Figure 22 shows isolated frames of the two camera views focused on the head/chest (left) and pelvis/lower extremities (right) in the time-zero frame (A), during contact (B), and during rebound (C). The stirrups of the litter poles separated from the litter pan, as seen in Figure 22C, and re-contacted the litter pan several times as the pulse progressed. There were no elongations and/or abrasions to the restraint webbing noted.

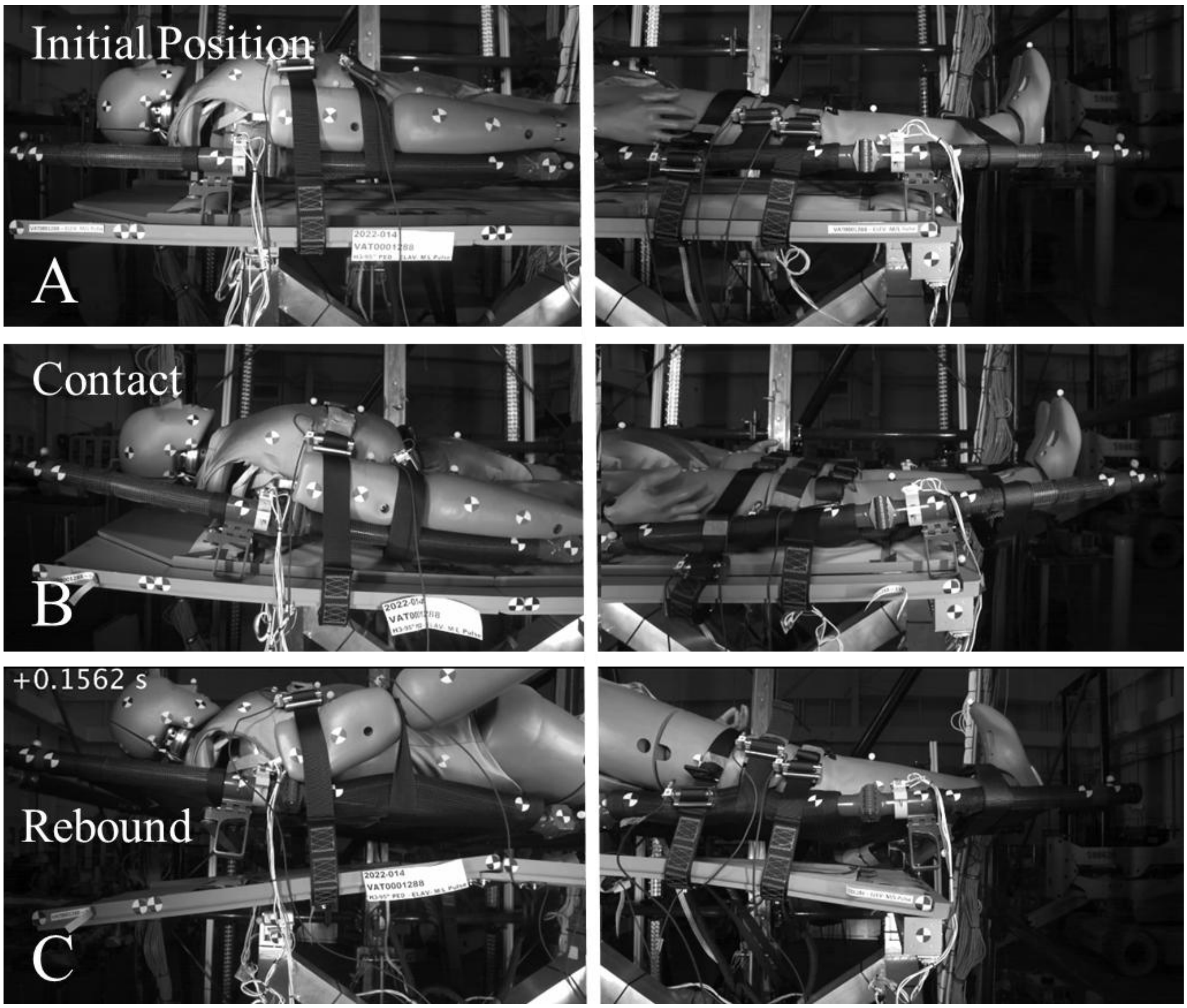

Figure 26. Views from the two HSV cameras centered on the head/chest (left) and pelvis/lower extremities (right) were combined for the 23 G pulse. The time-zero frame (A), frame where contact was observed (B), and the frame showing the rebound of the ATD (C) were selected from the HSV data for the elevated APMS.

This space is intentionally blank.

The graphite paper that lined the surface beneath the ATD and litter confirmed contact for all tests (Figure 23). Figure 23 shows contact of the chest, pelvis, and knees during the medium (23 G) pulse. The head did not contact the elevated litter pan, but both spreader bars under the litter did make contact.

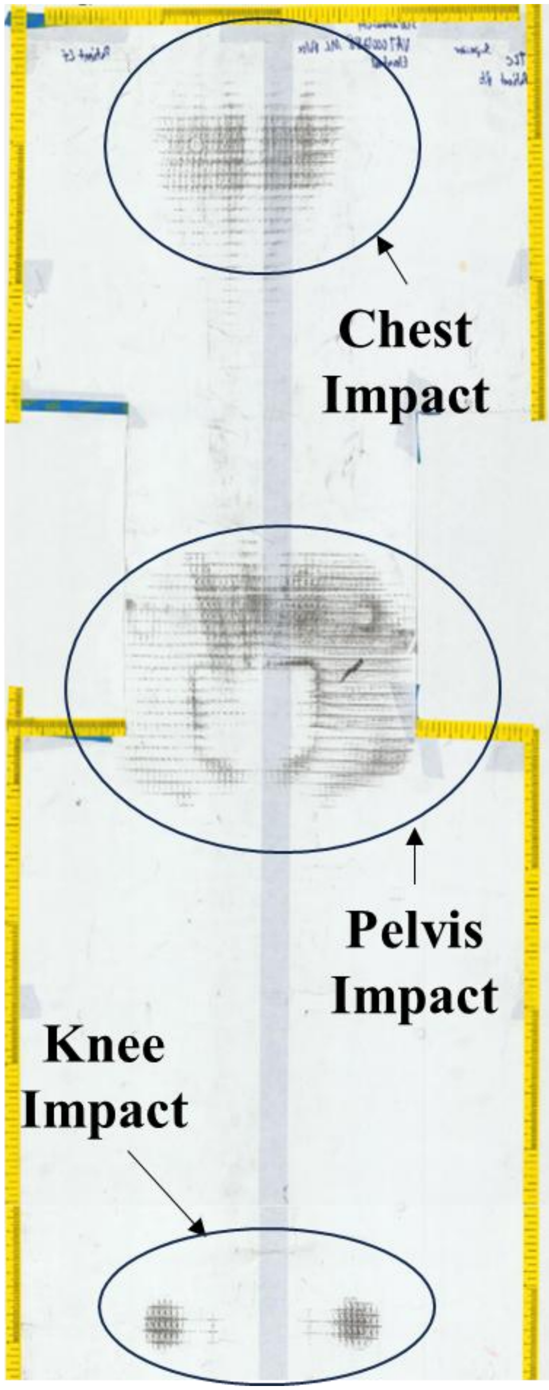

Figure 27. The ATD made contact with the litter pan during all pulses (imprint after one of the 23 G pulse is shown).

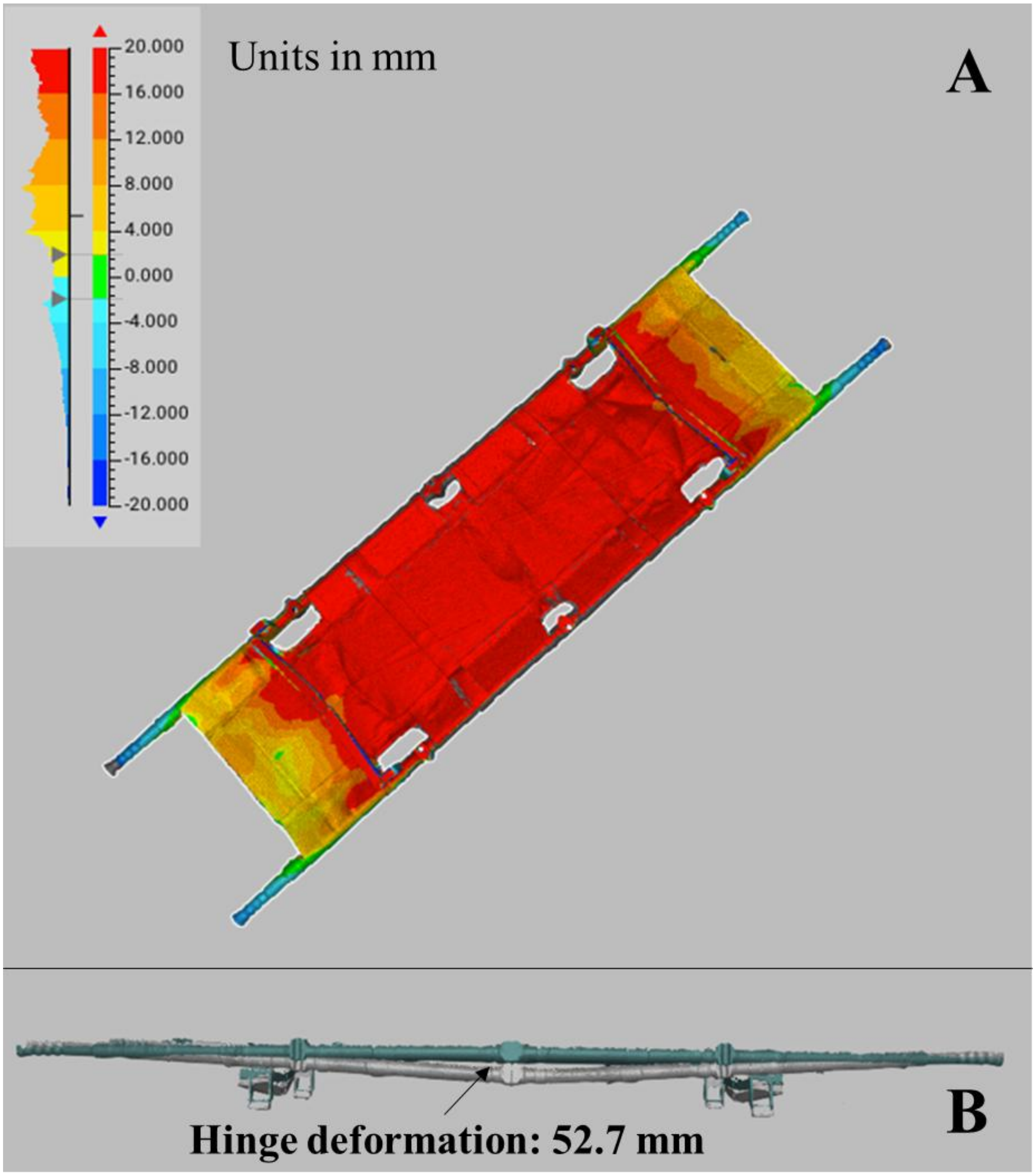

Figure 28. Bottom view (A) and side view (B) scans of the litter were taken of the elevated APMS litter bottom to document canvas and component deformation after one of the 23 G pulses. Units of deformation in the legend are in millimeters.

This space is intentionally blank.

Photos of the elevated APMS spreader bars were taken on the head and foot ends for comparison before and after testing (Figure 25). The post-test inspection noted deformations in the spreader bars at the head and foot for all tests, but the deformations were more pronounced after the 23 G pulse. There was also splaying of the stirrups laterally (left and right of the patient). There was no deformation to the litter pan or the forward and aft litter pan support (Figure 6), however, the pins of the litter pan support deformed slightly after the 23 G pulse (Figure 26). Although the spreader bars deformed, the litters could be collapsed and folded, and then re-opened and locked.

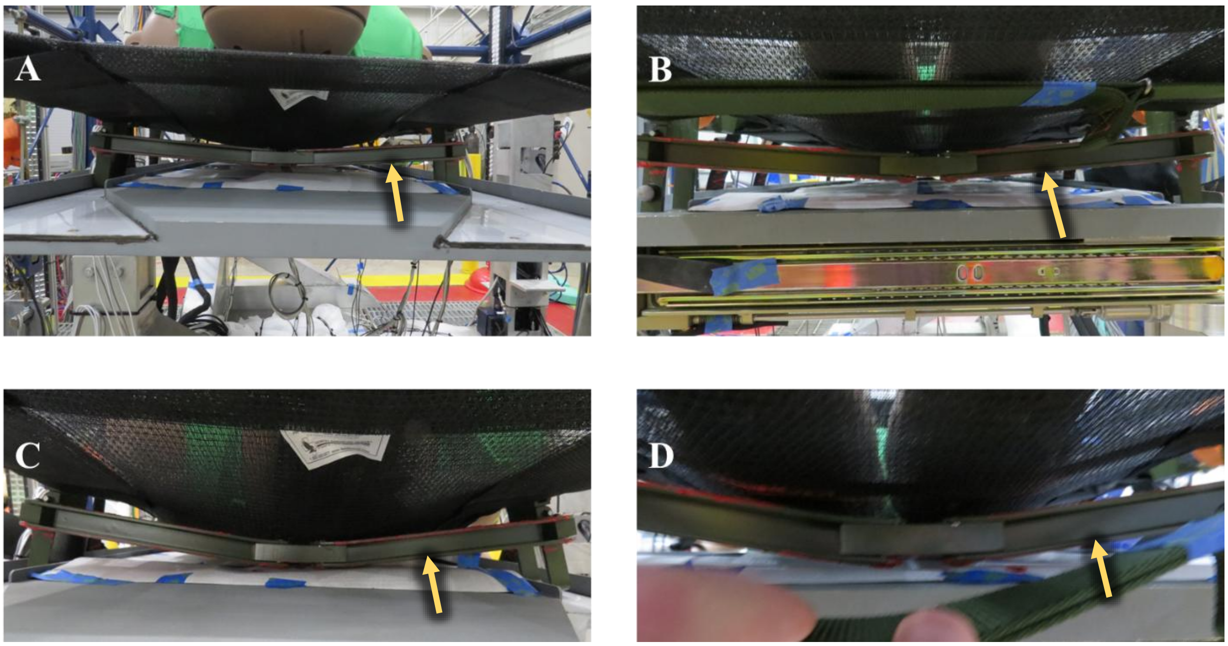

Figure 29. Pre-test photographs show the intact elevated APMS spreader bars of the head (A) and foot (B). Deformation of the head (C) and foot (D) spreader bars after the medium pulse were noted.

This space is intentionally blank.

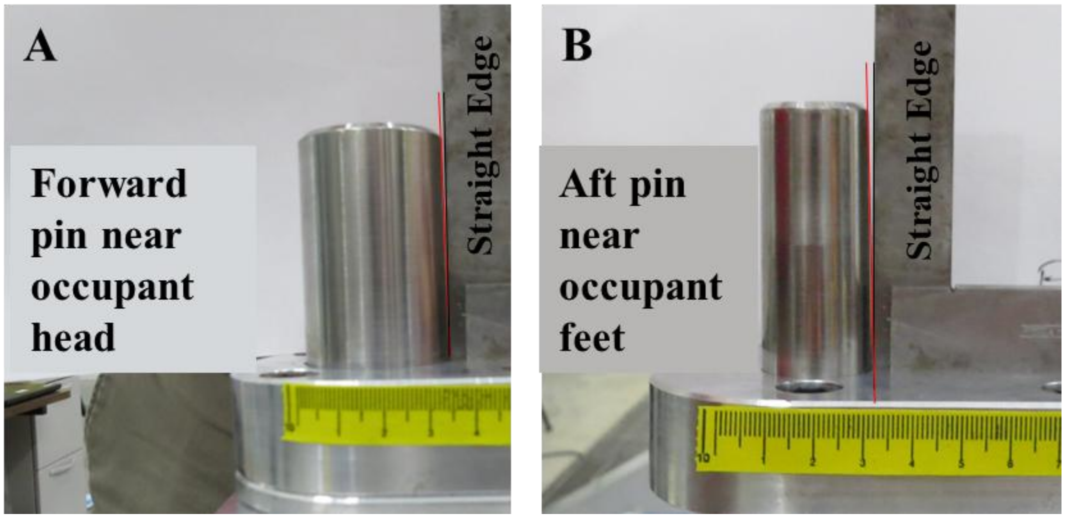

Figure 30. A straight edge was used to note pin deformation in the forward and aft litter pan support after the 23 G pulse. The red line shows the deformation from the straight edge.

This space is intentionally blank.

.

Discussion

Patients being aeromedically evacuated need to have crashworthy APMS that will mitigate the risk of acceleration-induced injury during a mishap. Litter occupants have the potential of impacting the floor, litter pan, or patient below during a mishap, potentially turning an injury into a fatality. The force needed to deflect the litter poles 12 inches was measured to be over 1000 lb by the Logsdon et al. (2015) litter study. Although Logsdon et al. (2015) found that the litter met the static performance requirements, the researchers also reported a concern that the occupant would contact the metal pan in a survivable crash, potentially causing [further] injury. The current study further substantiates these conclusions by demonstrating that, while minimal deflection of the litter poles was noted, the ATD contacted the simulated aircraft floor and litter pan at a crash pulse much lower than that of a survivable crash pulse. The current study demonstrated that contact of the ATD with the simulated aircraft floor and litter pan was made as a result of displacement through the webbing, the splaying of the stirrups laterally (left and right of the patient), and the deformation of the spreader bars and hinges.

The HIII-95M-PED was selected to conduct the current study due to its revised pelvis design that allowed the legs to rotate from a seated to a supine position and heavier body weight to challenge the structural integrity of the tested APMS components during dynamic testing. However, during the test setup, it was noticed that both rigid shoulder brackets of the ATD rested on the litter poles, which would have artificially supported the chest of the ATD on the litter poles rather than on the webbing. This was deemed a poor representation of how a Soldier of this size would interface with the litter; therefore, the ATD arms were disarticulated, and the shoulder brackets were removed to induce a more realistic representation where the litter webbing supported the chest during vertical loading. The HIII-50M-PED may be more appropriate for match-paired testing in dynamic tests. It is recommended that the HIII-95M-PED be used for static testing.

The Talon II 90C selected for this study had a hinged litter pole construction, which was deemed more vulnerable at higher accelerative exposures. However, the flexing of the litter pan hinge and deformation of the litter pole hinges, webbing, and support arm pins may have provided energy attenuation, resulting in lower accelerations imparted to the ATD chest and pelvis. It is recommended that the elevated APMS configuration with hinged litter poles be tested at high exposures to ensure that the system maintains integrity. It is also recommended that future testing include rigid litter poles to determine their structural integrity and ability to attenuate energy to the ATD.

This space is intentionally blank.

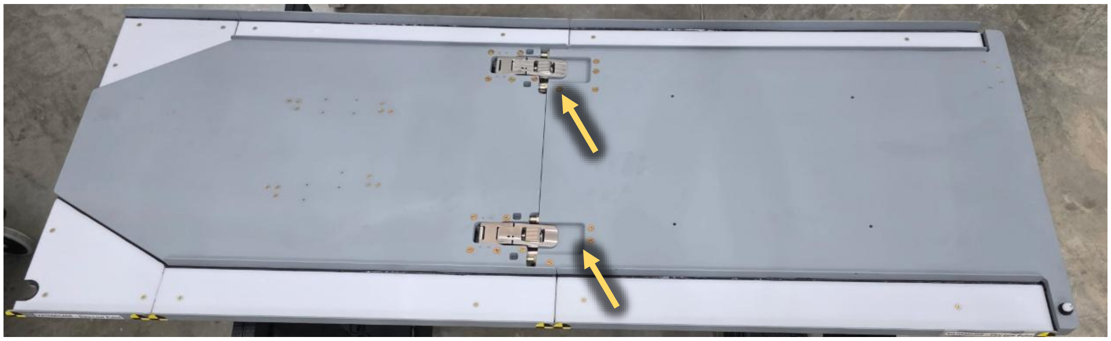

Figure 31. The elevated litter pan has a hinged construction (arrows).

The medium pulse target was 20 G for both APMS configuration tests. During pulse development, the VAT carriage was ballasted with rigid weights attached. However, during test executions, the occupant was suspended above the carriage by the distensible litter webbing. This gap allowed the carriage to be initially driven, decoupling the occupant mass resulting in a narrow time period where the carriage acceleration exceeded the target. Future testing at higher severities should consider this detail when developing a pulse.

Although the dynamic vertical test parameters in the current study were well below the guidance set forth in the ACSDG for APMS, notable deformation of the litter and impact of the ATD chest, pelvis, and knees with the structures beneath the litter were observed. The medium 23 G pulse used in the floor-mounted and elevated APMS configurations is less than 50% of the 48 G pulse recommended by the ACSDG. Additionally, the velocity change of the pulse (25 ft/s), another representation of severity, was about 35% of the ACSDG guidance of 42 ft/s. It remains uncertain if the floor-mounted and elevated APMS component will remain structurally intact at higher impact severities. Proceeding to a higher severity pulse should be approached with extreme caution considering the deformation to the litter and ATD sensor data noted under the 7G and 23 G pulses. It is recommended that conservative increases in severities be considered.

Litter pole instrumentation for each pulse revealed an initial delay in acceleration compared to the carriage acceleration for both floor and elevated configurations. This was attributed to the yielding of structures in the load path. For the floor-mounted configuration, these structures were primarily the litter stirrups. For the elevated configuration, these structures included the litter pan support arm, the hinged litter pan, and the litter stirrups. Additionally, the increased delays noted in both pulses for the elevated configuration were attributed to the greater flexibility of the cantilevered design. This was especially apparent as the litter poles furthest away (patient right) demonstrated the greatest initial delay compared to the litter poles nearest the supporting simulated airframe (patient left).

The stirrups of the litter poles leave the floor and re-contact the floor several times as the event progresses for both configurations. Striking the surface below the litter may further injure the occupant. It is recommended that affixing the stirrups to the surface below the litter be considered.

Each test resulted in the ATD contacting the floor or litter pan of their respective APMS. The ATD sensor data in the floor-mounted APMS recorded the highest acceleration in the pelvis followed by the chest and head. The ATD sensor data in the elevated APMS recorded the highest acceleration in the chest, followed by the head and pelvis. The resulting imprint the ATD left on the graphite paper was more prominent during the 23 G pulse of the elevated APMS than the floor-mounted APMS. The authors postulate that this was because the hinged construction of the litter pan in the elevated APMS (Figure 27) prevented the litter from displacing as far as the litter in the floor-mounted APMS. The litter pan also rests on a cantilever that appeared to flex in the HSV, causing the ATD to contact the surface below the litter multiple times. Graphite paper also performs better to shear forces, so the ATD may have slid as it made contact with the surface. Contact of the head with the surface below the litter could not be confirmed in the HSV or on the graphite paper for either APMS configuration; however, the head was positioned over one of the spreader bars which contacted the surface below it in all tests. It is possible that the head contacted the spreader bar. Consequently, floor-mounted and elevated APMS may need different static and dynamic requirements to ensure structural integrity and patient safety during mishaps. Future testing should incorporate HSV at the head and foot of the litter to capture the head and knees making contact with either the surface or the spreader below them.

More research should be conducted on the biofidelity of the ATD when loaded in the supine position from posterior to anterior. The spherical prominence of the posterior aspect of the straightened knees are in question. Also, in all 23 G tests, an unexpected and high magnitude moment about the y-axis (forward bending) was noted in the loading phase of both ATD femurs. An HSV review revealed the high magnitude to be temporally coincident with the posterior aspect of the ATD pelvis striking the surface below the litter. It is believed the measured femur moments about the y-axis are an artifact under supine posterior to anterior loading. It is recommended that post-mortem human subject subjects (PMHS) and matched-pair testing be conducted.

The current study revealed the flexibility of the litter mesh allowing the patient to impact the aircraft floor or litter pan, which may lead to injury. This indicates the need to conduct a comprehensive APMS human injury risk study with PMHS under similar conditions. It is possible to leverage particular parts of previous research to provide insight into the potential injury risk for litter patients. For example, injury risk curves developed for rear blunt head impact injury (Daniel et al., 2022) or the “Human Tolerance to Rapidly Applied Acceleration Assessment” conducted by NASA (Eiband, 1959) could be applied to litter patients; however, the unique position of a litter patient could limit applicability. Litter patients are typically in a supine position with legs straight, which is unusual in injury biomechanics as this is a relatively rare position of a vehicle occupant. It is recommended that a two-phased approach to researching litter occupant injury risk using PMHS be used. In the first phase, a PMHS and matched-pair testing should be conducted starting at a lower severity. The results of the first phase will inform on vulnerable body regions for litter occupants and provide information for injury risk curve development. In the second phase, a PMHS study should be conducted with the PMHS on a rigid surface and tested at the injurious pulse identified in the first phase of the study to ensure injuries were not a result of the applied acceleration but from the APMS.

In addition to conducting injury risk research for APMS in the vertical direction, there is a need for dynamic loading performance requirements that assess the structural integrity of APMS during a crash event and assesses the risk to the patient/occupant in multiple loading scenarios. This study did not consider lateral or longitudinal impact directions versus lateral verses longitudinal APMS. These loading scenarios should be considered. Test requirements should also include appropriate occupant weights across current population percentiles to address injury risk for the entire modern Soldier population.

Dynamic loading performance requirements should be developed to include mitigating severe occupant contact with occupants or rigid structures above or below. Minimum instrumentation should consider an accelerometer on the carriage, 6DOF on the litter poles above each stirrup, and the standard HIII-50M-PED instrumentation package. The low severity 7 G pulse did not sufficiently challenge the APMS, therefore, the 23 G, 25 ft/s pulse is recommended for initial testing. Test results should produce no structural collapse or loss of integrity of the APMS. If no PMHS injuries are produced, it is recommended to increase the severity of the pulse.

Conclusion

The development, and subsequent implementation, of a dynamic test standard for APMS will improve patient safety during aeromedical transport and allow the Future Vertical Lift program to mitigate patient injury risk through improved APMS crashworthiness. Preliminary data resulting from this study demonstrated a need for an APMS dynamic testing requirement. Furthermore, floor-mounted and elevated APMS may need to be evaluated differently due to differences in construction. It is recommended to incorporate interim dynamic loading performance requirements into the development of acquisition requirements for future APMS so that already vulnerable litter patients will be better protected in dynamic impacts. Future work should include dynamic APMS tests in multiple loading scenarios with PMHS to assess ATD biofidelity in the supine position with occupant weights across current Soldier population percentiles.

Recommendations

The outcomes of this research led to the following recommendations:

- A static and dynamic test standard for APMS assessment should be developed for multiple loading conditions (i.e., vertical, longitudinal, and lateral).
- The HIII-95M-PED is recommended for static litter performance requirements.
- The HIII-50M-PED is recommended for dynamic litter performance requirements.
- At a minimum, the acceleration pulse for the APMS vertical dynamic test should be 23 G at a velocity of 25 ft/s.
- Minimum instrumentation should consider an accelerometer on the carriage, 6DOF on the litter poles above each stirrup, and the standard HIII-50M-PED instrumentation package.
- It is recommended that securing the stirrups to the surface below the litter be considered.

- Additional research should be conducted to develop injury risk criteria for supine occupants transported in APMS.

References

Annett, M. S., Littell, J., Jackson, K. E., Bark, L. W., DeWeese, R. L., & McEntire, B. J. (2014). *Evaluation of the first transport rotorcraft airframe crash testbed (TRACT 1) full-scale crash test* (TM-2014-218543). National Aeronautics and Space Administration.

Annett, M., & Littell, J. (2015). *Evaluation of the second transport rotorcraft airframe crash testbed (TRACT 2) full scale crash test* (Report No. NF1676L-19737). In AHS International Annual Forum.

Daniel, R., Tooks, R., Gomez, J., Fralish, V., Logsdon, K., McGovern, S., Chancey, V.C., & Brozoski, F. (2022). *Evaluation of skull fracture risk association with helmet back-face deformation* (Report No. USAARL-TECH-FR--2022-24). U.S. Army Aeromedical Research Laboratory.

Department of the Army. (1991). *Medical evacuation in a theater of operations: Tactics, techniques, and procedures* (Field Manual 8-10-6). Headquarters, Department of the Army.

Department of the Army. (2018). *The U.S. Army in multi-domain operations 2028* (Pamphlet 525-3-1). U.S. Army Training and Doctrine Command.

Desjardins, S. P., Zimmerman, R. E., Bolukbasi, A. O., & Merritt, N. A. (1989). *Aircraft crash survival design guide, Volume IV – Aircraft seats, restraints, litters, and cockpit/cabin delethalization* (USAAVSCOM TR 89-D-22D). Aviation Applied Technology Directorate.

DoD. (1987). *Airplane strength rigidity miscellaneous loads* (Military Standard MIL-A-8865B[AS]). U.S. Department of Defense.

DoD. (1997). *Litter, folding, rigid pole, decontaminable* (MIL-L-49511B). U.S. Department of Defense.

Dorland P., & Nanney J. (1982). *Dust off: Army aeromedical evacuation in Vietnam*. Center of Military History, United States Army.

Eiband, M. (1959). *Human tolerance to rapidly applied accelerations: A summary of the literature* (NASA MEMO 5-19-59E). Lewis Research Center. https://ntrs.nasa.gov/api/citations/19980228043/downloads/19980228043.pdf

Gordon, C. C., Blackwell, C. L., Bradtmiller, B., Parham, J. L., Barrientos, P., Paquette, S. P., Corner, B. D., Carson, J. M., Venezia, J. C., & Kristensen, S. (2014). *2012 anthropometric survey of U.S. Army personnel: Methods and summary statistics* (Report No. NATICK/TR-15/007). U.S. Army Natick Soldier Research Development and Engineering Center.

Logsdon, K. P., Fralish, V. R., Brozoski, F. T., Licina, J. R., Bowers, B. L., & Chancey, V. C. (2015). *A novel quasi-static evaluation of military medical litter load performance* (Report No. USAARL-2015-13). U.S. Army Aeromedical Research Laboratory.

McEntire B. J., Weisenbach C. A., Bowman, T., Fralish, V., & Holderfield, M. (2016, April 24-28). *Occupant response in an improved patient litter system during a full-scale CH-46 crash test* [Presentation]. 87th Aerospace Medical Association Annual Meeting, Atlantic City, NJ.

National Transportation Safety Board. (1980). *Safety report - The status of general aviation aircraft crashworthiness* (NTSB-SR-80-2). National Transportation Safety Board.

Rhodes, D., McEntire, B. J., Ballard, M. T., & Chancey, V. C. (2021). *Implications of updated soldier anthropometry and gear weights on future and enduring seating based on the UH-60 crew chief/gunner and medic seat retention strength* (Report No. USAARL-2021-52). U.S. Army Aeromedical Research Laboratory.

SAE International. (2007). *Instrumentation for impact test—Part 1—Electronic instrumentation* (J211/1_200707). SAE International.

Schamadan J., Turnbow J. W., & Weinberg L. W. T. (1963). *Dynamic test of an aircraft litter installation one of a series of reports pertaining to the dynamics crash test of a U.S. Army H-21 helicopter* (Technical Report 63-3). Transportation Research Command.

Turnbow, J. W., Carroll, D. F., Haley, J. L., Reed, W. H., Robertson, S. H., & Weinberg, L. W. T. (1967). *Crash survival design guide* (USAAVLABS TR 67-22). U.S. Army Air Mobility Research and Development Laboratory.

U.S. Army Medical Department Center & School. (2019). *AMEDD white paper, concept for medical operations and support*.

Weinberg, L. W. T. (1966). *Aircraft litter retention system design criteria* (Technical Report 66-27). U.S. Army Aviation Materiel Laboratories.

Weisenbach, C. A., Rooks, T., Bowman, T., Fralish, V., & McEntire, B. J. (2017). Patient litter system response in a full-scale CH-46 crash test. *Military Medicine, 182*(suppl_1), 287–294.

Appendix

Table A1. Peak ATD Accelerations for the Head, Chest, and Pelvis in the *x*-Axis Direction for the Floor-Mounted APMS Configuration

	A*x* (G)		
Pulse	Head	Chest	Pelvis
7 G	16.5	17.1	26.8
7 G	15.8	16.6	26.8
7 G	15.2	21.2	34.9
23 G	42.5	112.7	145.6
23 G	39.8	131.5	163
23 G	41.8	134.8	170.2

Table A2. Peak ATD Right and Left Femur Load Cell Force in the *x*-Axis Direction for the Floor-Mounted APMS Configuration

	Fx (lb)		**My (in-lb)**	
Pulse	Right Femur	Left Femur	Right Femur	Left Femur
7 G	45.5	46	1718.2	1788.4
7 G	55.9	58.4	1687.4	1639.6
7 G	115.9	77	1209.7	1791.4
23 G	632.1	620	4084.1	3973.3
23 G	678.5	651.6	4082.3	3963.2
23 G	771	734.6	4086.1	4097.6

This space is intentionally blank.

Table A3. Peak ATD Accelerations for the Head, Chest, and Pelvis in the *x*-Axis Direction for the Elevated APMS Configuration

	Ax (G)		
Pulse	Head	Chest	Pelvis
7 G	13.8	12.6	15.8
7 G	12.6	12.7	15.5
7 G	13.6	12.9	15.7
23 G	52.7	86.3	47
23 G	65.1	104.6	43.9
23 G	57.6	103.2	46.4

Table A4. Peak ATD Right and Left Femur Load Cell Force in the *x*-Axis Direction for the Elevated APMS Configuration

	Fx (lb)		**My (in-lb)**	
Pulse	Right Femur	Left Femur	Right Femur	Left Femur
7 G	63.1	67.5	832.7	890
7 G	49	41.3	579.7	645.8
7 G	71.4	69.7	897	1062.3
23 G	217.8	268.8	2635.7	2701.5
23 G	257.3	258.2	2592.9	2293
23 G	267.3	259.5	2988.1	2719

This space is intentionally blank.

U.S. ARMY AEROMEDICAL RESEARCH LABORATORY

FORT RUCKER, ALABAMA

Optimizing

HUMAN PROTECTION AND PERFORMANCE

since 1962

U.S. ARMY

FCC

MRDC